

January 2014

# Impedance Extraction by MATLAB/Simulink and LabView/Multisim

Jen-Pin Lin

*University of South Florida, [jenpin@mail.usf.edu](mailto:jenpin@mail.usf.edu)*

Follow this and additional works at: <http://scholarcommons.usf.edu/etd>



Part of the [Electrical and Computer Engineering Commons](#), and the [Oil, Gas, and Energy Commons](#)

---

## Scholar Commons Citation

Lin, Jen-Pin, "Impedance Extraction by MATLAB/Simulink and LabView/Multisim" (2014). *Graduate Theses and Dissertations*.  
<http://scholarcommons.usf.edu/etd/5257>

This Thesis is brought to you for free and open access by the Graduate School at Scholar Commons. It has been accepted for inclusion in Graduate Theses and Dissertations by an authorized administrator of Scholar Commons. For more information, please contact [scholarcommons@usf.edu](mailto:scholarcommons@usf.edu).

Impedance Extraction by MATLAB/Simulink and LabView/Multisim

by

Jen-Pin Lin

A thesis submitted in partial fulfillment  
of the requirements for the degree of  
Master of Science in Electrical Engineering  
Department of Electrical Engineering  
College of Engineering  
University of South Florida

Co-Major Professor: Lingling Fan, Ph.D.  
Co-Major Professor: Zhixin Miao, Ph.D.  
Chung Seop Jeong, Ph.D.

Date of Approval:  
April 17, 2014

Keywords: Power Injection, D-Q Transform, Power Electronics, IPFFT, Measurement Algorithm Design

Copyright © 2014, Jen-Pin Lin

## **Dedication**

To my parents for never failing to give me financial and moral support, for giving me all I need during the time I developed my system, and for teaching me that even the largest task can be accomplished if it is done one step at a time.

## **Acknowledgments**

I would like to thank my colleagues at the Smart Grid Power Systems Laboratory (SPS). I have had many conversations and investigated many tough questions with many of them. Everyone is my valuable resource to the power community.

I would like to thank my committee members, Dr. Chung Seop Jeong-I appreciate your help and the time you have given me in helping me during my studies.

I would like to thank Dr. Zhixin Miao for his continual help and support throughout my time in SPSS. Zhixin has given me lots of help and advice during my time in University of South Florida as a project member and as a committee member.

I would like to give special thanks to my advisor, Dr. Lingling Fan. It is with her help and support that I have been able to complete this project. Dr. Fan has been my first course professor since I've been to USF, and is my advisor for my Master's degree.

I would like to thank my friends and family for always being there and supporting me!

## Table of Contents

List of Tables . . . . .	iii
List of Figures . . . . .	iv
Abstract . . . . .	viii
Chapter 1 Introduction . . . . .	1
1.1 Dynamics of Three Phase Systems Under Active Loads . . . . .	1
1.2 System Stability Analysis in DQ Coordinates . . . . .	2
1.2.1 Objective Statement . . . . .	4
1.3 Review of Existing Technologies . . . . .	4
1.4 Summary . . . . .	5
1.5 Thesis Contents . . . . .	5
Chapter 2 Impedance Extraction Algorithm . . . . .	7
2.1 Model Description . . . . .	7
2.1.1 Voltage Injected Model Description . . . . .	7
2.1.2 Current Injected Model Description . . . . .	11
2.2 Impedance Calculation Method . . . . .	16
2.2.1 Injection Restriction . . . . .	17
2.3 Injection Concept . . . . .	19
2.3.1 Injected Voltage Selection . . . . .	19
2.3.2 Injected Current Selection . . . . .	21
Chapter 3 MATLAB Algorithm Architect . . . . .	23
3.1 Model Description and Parameters . . . . .	23
3.2 Phase-Locked Loop . . . . .	26
3.2.1 Design Principle and Effects . . . . .	26
3.2.2 PLL Designed by MATLAB/Simulink . . . . .	27
3.3 DQ Transform With Voltage Perturbation . . . . .	29
3.4 Interpolated Fast Fourier Transformation . . . . .	31
3.4.1 Demand of Using IPFFT . . . . .	31
3.4.2 Algorithm of Interpolated FFT . . . . .	32
3.4.3 Example of Interpolated FFT . . . . .	34
3.5 Simulation Results by MATLAB/Simulink/Simpower . . . . .	38
3.6 Case Study: AC/DC/AC Converter . . . . .	41

Chapter 4	Impedance Extraction Algorithm Architect by LabView and Multisim . . . . .	47
4.1	Multisim Circuit Model and Configuration . . . . .	47
4.2	LabVIEW Algorithm Architect . . . . .	48
4.2.1	Parallel Programming Output . . . . .	48
4.2.2	Phase-Locked Loop and Ramp Signal . . . . .	49
4.2.3	Park Transform . . . . .	50
4.3	Results and Analysis . . . . .	52
4.4	Case Study . . . . .	58
4.5	Summary and Conclusions . . . . .	65
Chapter 5	Summary and Conclusions . . . . .	66
5.1	Summary . . . . .	66
5.2	Conclusions . . . . .	66
5.3	Future Work and Improvements . . . . .	67
5.3.1	Controllable Voltage or Current Source . . . . .	67
5.3.2	Algorithm Implementation . . . . .	69
References	. . . . .	70
About the Author	. . . . .	End Page

## List of Tables

Table 1	Simple Circuit Parameters . . . . .	24
Table 2	Parameter Definitions . . . . .	32
Table 3	Parameter for AC/DC/AC Converter . . . . .	42
Table 4	RL Circuit Parameters . . . . .	48
Table 5	AC to DC Rectifier Parameters . . . . .	59
Table 6	DC to AC Inverter Parameters . . . . .	62

## List of Figures

Figure 1	Three-Phase AC Balanced Waveform . . . . .	1
Figure 2	Constant Power Characteristic . . . . .	2
Figure 3	Three-Phase AC Balanced Circuit with Injected Voltages . . . . .	7
Figure 4	Single-Phase AC Circuit . . . . .	8
Figure 5	Transformed Single-Phase Circuit . . . . .	8
Figure 6	Transformed Three-Phase Circuit . . . . .	9
Figure 7	System in DQ Reference Frame . . . . .	9
Figure 8	Impedance Model in DQ System . . . . .	10
Figure 9	First Injection in System for DQ Reference Frame . . . . .	10
Figure 10	Second Injection in System for DQ Reference Frame . . . . .	11
Figure 11	Frequency Domain for DQ Coordinate Circuit . . . . .	12
Figure 12	Three-Phase AC Balanced Circuit with Injected Currents . . . . .	12
Figure 13	Transformed Three-Phase Circuit with Injected Currents . . . . .	13
Figure 14	System in D-Q Coordinate . . . . .	13
Figure 15	Impedance Model in D-Q Coordinate . . . . .	14
Figure 16	First Current Injection in DQ Reference Frame . . . . .	14
Figure 17	Second Current Injection in DQ Reference Frame . . . . .	15
Figure 18	Frequency Domain in D-Q Reference Frame . . . . .	15
Figure 19	Vector Diagram of Injected Voltages in D-Q Frame . . . . .	21
Figure 20	Simulation RL Circuit in Simpower . . . . .	24
Figure 21	Source Voltage Scope in Simulink . . . . .	24



Figure 22	Ideal Voltage Controlled Source . . . . .	25
Figure 23	Load Voltage Scope in Simulink . . . . .	25
Figure 24	Block Diagram of Phase-Locked Loop . . . . .	26
Figure 25	Phase-Locked Loop Design in MATLAB/Simulink . . . . .	27
Figure 26	Ramp Signal By MATLAB/Simulink . . . . .	28
Figure 27	Source Voltage Transformed in DQ Reference Frame . . . . .	28
Figure 28	Sinusoidal Fluctuation in D-Axis . . . . .	29
Figure 29	Clear Sinusoidal Fluctuation in D-Axis . . . . .	30
Figure 30	Sinusoidal Fluctuation in Q-Axis . . . . .	30
Figure 31	Clear Sinusoidal Fluctuation in Q-Axis . . . . .	31
Figure 32	IPFFT Analysis for First 0.5 Second . . . . .	34
Figure 33	IPFFT Analysis in DQ Reference Frame . . . . .	35
Figure 34	IPFFT Analysis in $V_{d1}$ . . . . .	36
Figure 35	IPFFT Analysis in $V_{d2}$ . . . . .	36
Figure 36	IPFFT Analysis in $I_{d1}$ . . . . .	37
Figure 37	IPFFT Analysis in $I_{d2}$ . . . . .	37
Figure 38	Actual Impedance Model in Real Part . . . . .	38
Figure 39	Actual Impedance Model in Imaginary Part . . . . .	39
Figure 40	Impedance Results $Z_{sdd}$ . . . . .	39
Figure 41	Impedance Results $Z_{sqq}$ . . . . .	40
Figure 42	Impedance Results $Z_{ldd}$ . . . . .	40
Figure 43	Impedance Results $Z_{lqq}$ . . . . .	41
Figure 44	AC to DC to AC Converter Circuit Diagram . . . . .	41
Figure 45	Voltage Injection for AC/DC/AC Converter . . . . .	43
Figure 46	Voltage Measurement after Disturbance . . . . .	43

Figure 47	Output of AC/DC/AC Converter . . . . .	44
Figure 48	$Z_{sdd}$ for AC/DC/AC Converter . . . . .	44
Figure 49	$Z_{sqq}$ for AC/DC/AC Converter . . . . .	45
Figure 50	$Z_{ldd}$ for AC/DC/AC Converter . . . . .	45
Figure 51	$Z_{lqq}$ for AC/DC/AC Converter . . . . .	46
Figure 52	RL Circuit Built by Multisim . . . . .	47
Figure 53	LabVIEW I/O Interface with Multisim . . . . .	49
Figure 54	Phase-Locked Loop in LabVIEW . . . . .	49
Figure 55	Ramp Signal Created by LabVIEW . . . . .	50
Figure 56	Ramp Signal Result in LabVIEW . . . . .	50
Figure 57	Park Transformation in MathScript . . . . .	50
Figure 58	Ramp Signal Algorithm in LabVIEW . . . . .	51
Figure 59	$V_d$ and $V_q$ After Park Transform . . . . .	51
Figure 60	Three-Phase Balanced Voltage Source . . . . .	52
Figure 61	Load Voltages with Disturbance . . . . .	53
Figure 62	$V_d$ and $V_q$ . . . . .	53
Figure 63	$V_d$ and $V_q$ in Detail . . . . .	54
Figure 64	$I_d$ and $I_q$ . . . . .	54
Figure 65	$I_d$ and $I_q$ in Detail . . . . .	55
Figure 66	Actual Impedance Model in Real Part . . . . .	55
Figure 67	Actual Impedance Model in Imaginary Part . . . . .	56
Figure 68	$V_{sdd}$ Impedance Model . . . . .	56
Figure 69	$V_{sqq}$ Impedance Model . . . . .	57
Figure 70	$V_{ldd}$ Impedance Model . . . . .	57
Figure 71	$V_{lqq}$ Impedance Model . . . . .	58

Figure 72	Impedance Extraction Algorithm . . . . .	58
Figure 73	AC to DC Rectifier Circuit Diagram . . . . .	59
Figure 74	$V_{sdd}$ Impedance Model for AC/DC Rectifier . . . . .	60
Figure 75	$V_{sdq}$ Impedance Model for AC/DC Rectifier . . . . .	60
Figure 76	$V_{sqd}$ Impedance Model for AC/DC Rectifier . . . . .	61
Figure 77	$V_{sqq}$ Impedance Model for AC/DC Rectifier . . . . .	61
Figure 78	DC to AC Inverter Circuit Diagram . . . . .	62
Figure 79	$V_{sdd}$ Impedance Model for DC/AC Inverter . . . . .	63
Figure 80	$V_{sdq}$ Impedance Model for DC/AC Inverter . . . . .	63
Figure 81	$V_{sqd}$ Impedance Model for DC/AC Inverter . . . . .	64
Figure 82	$V_{sqq}$ Impedance Model for DC/AC Inverter . . . . .	64
Figure 83	Back-to-Back Inverter Research Board with Load . . . . .	68

## **Abstract**

This thesis studies the techniques of small-signal impedance measurement in three-phase power systems. Stability issue has become critically important since power electronics are highly applied in power distribution and conversion systems. Controlled output systems cause the risk of instability. In order to obtain the impedance model, an impedance extraction in D-Q reference frame algorithm is developed. This paper also applied Interpolated Fast Fourier Transform to increase accuracy of impedance model. Based on the voltage injection, Phase-Locked Loop, Park Transform, D-Q reference frame, and IPFFT. Three-phase system has been realigned on D-Q coordinate and impedance model is extracted in this form.

Firstly, impedance extraction algorithm is designed by MATLAB/Simulink, the algorithm includes PLL, D-Q transform, and IPFFT is used to obtain magnitude and phase angle in frequency domain. Impedance matrices in D-Q frame may be solved through the relation between currents and voltages. Impedance model is made through various tests. Secondly, using the algorithm to test RL circuit to verify with real bode plot of the circuit. Then apply the algorithm on sophisticated circuit model. Finally, implement the algorithm on LabView/Multisim for future hardware tests.

This paper clearly describes the objective of the research, the research problem and approaches, and experiment setup. This paper presents work conducted at the Smart Grid Power Systems Laboratory at University of South Florida.

## Chapter 1

### Introduction

In a three-phase AC system, three circuit conductors carry three alternating currents which reach instantaneous peak values at one third of the cycle from each other, which means 120 degrees phase shift for each phase. Constant power has affected by the delay of phases with each other. The three-phase voltage or currents waveform forms sinusoidal patterns with 120 degrees as shown in FIG 1.

There are numerous materials used three-phase power in power electronics, based on the functions to provide power to loads, to provide filter, and convert energy forms. Examples are inverters, rectifiers, AC-AC converters, motor drives, and filters.

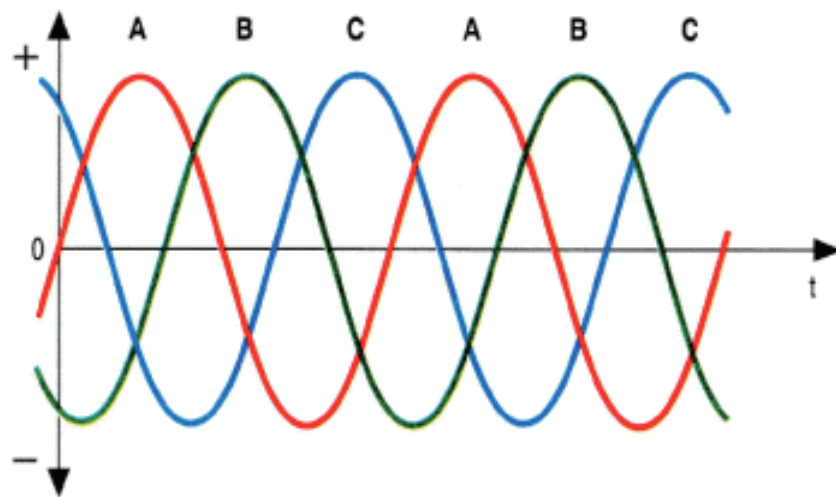


**Figure 1.** Three-Phase AC Balanced Waveform

### 1.1 Dynamics of Three Phase Systems Under Active Loads

Power electronics has been well-developed to apply in the power processing and generation field in contemporary electric power systems. Power electronic technology provides outstanding performance and can be applied closed loop control in the power systems, which means that the output of the power converter can

be regulated according to the requirement of the load. While the converters are not linear, the dynamics are affected by the load and source systems that they provide the power or consume the power. However, with this closed-loop regulation, some phenomena cannot be easily observed in the power system, the phenomena itself may threaten the stability of the power system. [1]

Reference [2] shown that systems based on power electronic are trend to negative impedance instability due to the constant-power feature of the components. Systems of power electronic control the output voltage. At a fixed current point, systems consume constant power. Even though power converter is ideal and lossless, the input power will also have a constant power feature as shown in Fig 2.

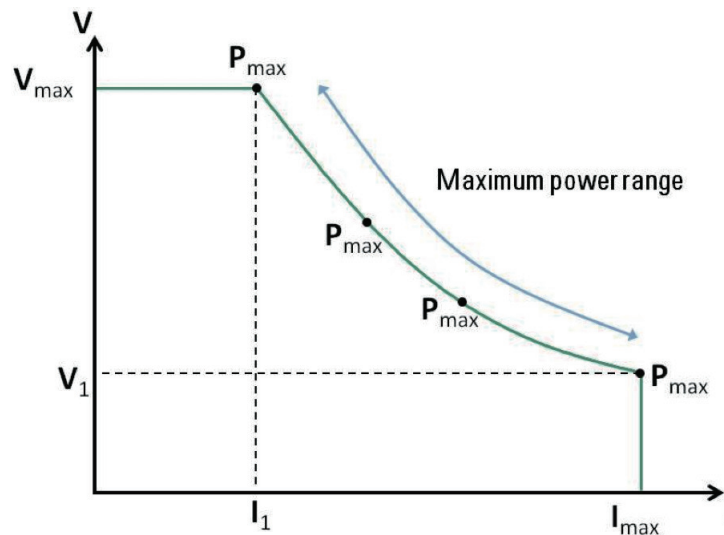


**Figure 2.** Constant Power Characteristic

A real world phenomenon, impedance-model-based subsynchronous resonance oscillations, has been studied to states the stability of power systems with resonance by controlling the control gain of rotor side converter. [3] Although some of large scale power grids can bear many of these characteristics since the effect is relatively limited because of the size of the system, several small-scale power grids can't tolerate these behaviors. Some small power grids have their own power system, those grids are not linked to the infinite buses directly. It is necessary to analyze the stability of systems for small power grids.

## 1.2 System Stability Analysis in DQ Coordinates

The power system uses closed-loop control to regulate the power which contains three-phase power converters. This report focuses on impedance extraction, which is doing impedance measurement based on

frequency. The model will be small signal system in order to show the power electronic and system behavior at a given operating point.

In power electronics systems, the loads tend to have dynamic properties, and the power conditioning equipment also has dynamic properties such as inductors and capacitors and some of the controllers introduce additional states and delays. The power converters themselves mostly comprise a set of nonlinear dynamics which contain discontinuous nonlinear differential equations. These systems are still hard to analyze although they have been simplified. For a regular three-phased voltage, the equation is given by (2.20) which owns periodic tendencies.

$$\begin{aligned} V_a &= V_m \cos(\omega_e t) \\ V_b &= V_m \cos(\omega_e t - 2\pi/3) \\ V_c &= V_m \cos(\omega_e t + 2\pi/3) \end{aligned} \tag{1.1}$$

The equation (1.1) clearly states that it is a three phase balance system with 120 degree phase delay for each phase. In order to arrange this non-stationary system into a stationary system, the transform of three phase system to simple DC component is needed. To pursue this goal, three phase voltages can be seen as three voltage vectors which are rotating in three-dimensional space. If we look at the voltage vector while we see the coordinate keep rotating in the frequency  $w$  radiance per second. Once the coordinate is rotating at the same speed as the three-phase voltage, the voltage vectors can stay stationary in the frame. The transformation function used in this report was Park Transformation, also called D-Q Transformation, the equation is shown as (1.2).

$$\begin{bmatrix} V_d \\ V_q \\ V_0 \end{bmatrix} = \frac{2}{3} \begin{bmatrix} \cos(\theta) & \cos(\theta - 2\pi/3) & \cos(\theta + 2\pi/3) \\ \sin(\theta) & \sin(\theta - 2\pi/3) & \sin(\theta + 2\pi/3) \\ 1/2 & 1/2 & 1/2 \end{bmatrix} \begin{bmatrix} V_a \\ V_b \\ V_c \end{bmatrix} \tag{1.2}$$

$V_0$  can be ignored as zero in this report since 0-axis stays always as zero in any kind of three-phase balanced system after the park transformation while all three phase can be canceled if each one is 120 degree lag.

In order to analyze a non-linear system, the operating point is needed to perform linear analysis. It is hard to do analysis if the system is unbalanced because of lacking an operating point. If the system is the balanced system as (2.20), which will be mentioned in chapter 2. By applying the system into Park

transform equation (1.2), the three-phased system can be transformed into DC system. (1.3) can be obtained by multiplying (2.20) and (1.2).

$$\begin{bmatrix} V_d \\ V_q \\ V_0 \end{bmatrix} = \sqrt{(2/3)} \begin{bmatrix} 3/2 \\ 0 \\ 0 \end{bmatrix} [V_m] \quad (1.3)$$

In (1.3), it states that in a balanced three-phased system and applies the same rotating frequency speed of rotating frame. The system can be seen as 2 DC components with average magnitude and zero voltage.

To analyze system stability, the system should be injected another power source to make a perturb the system. However, the injected power source should maintain a reliable energy to make a perturbation to the system and not to lead the system collapse. Since the injected voltage source has different frequency between the system, in D-Q coordinate can observe overlap waveform made by injected power source.

### 1.2.1 Objective Statement

The objective of this work is to do the impedance extraction based on D-Q reference frame through algorithm by using MATLAB/Simulink. After successfully analyzing impedance measurement, apply the technique on LabView/Multisim and further test with single board AC/DC/AC converter.

## 1.3 Review of Existing Technologies

The impedance measurement can be approached in several ways. First, non D-Q frame impedance measurement is applied by injected disturbance and collected several data points. [4] DC power supply impedance uses a similar idea to D-Q reference frame since the DC power doesn't include three-phase balanced voltages and currents, the disturbance can be observed online voltage and current. [5]

Single-phase impedance extraction has been done in [6]. Taking single-phase ac system DC to AC inverter as an example, current has injected between the load and inverter. Filter is necessary in order to get pure sinusoidal waveform of the current. Next, using park transform to obtain injected harmonic and further calculate impedance model. Reference [7]. [8]addresses impedance extraction by injecting line-to-line current and analysis the impedance model in D-Q reference frame. Using H-bridge based injection and chopper injection circuit to inject line-to-line current. This method is applied on AC synchronous machine connect to load by installing chopper circuit on Phase B and Phase C [9]. Three-phase AC current injection and



convert line voltage to D-Q reference frame to obtain impedance model is the other technique. The current injection is controlled by three-phase bridge inverter or three-phase chopper circuit which can change its frequency from  $1Hz$  to  $10kHz$ . [10] Finally, another way to get impedance model by one injection to DC or three-phase AC system is training recurrent neural network. [11]

The algorithm [12] is to measure one frequency at a time and calculate one impedance in assigned frequency then combine all of data to obtain impedance model. The algorithm introduced in detail includes how to design a Phase-Locked Loop, Park Transform, impedance matrices solution in frequency domain. Impedance measurement using chirp signal is proposed to solve the drawback of time-consuming of current injection method [13]. Impedance model can be obtained in one step by injecting chirp signal as a disturbance.

#### **1.4 Summary**

The need of knowing impedance measurement in AC systems is in high demand. System stability is more and more important for small power systems which own limited power generation capacity. In addition, the power electronics for small system will destabilize their host systems since the frequency changes in large range. The impedance extraction technique can measure more accurate system's impedance model, which is hard to obtain one by one in traditional way and negative impedance created by some power converters.

#### **1.5 Thesis Contents**

Chapter 1 has provided an introduction of the background of the three-phase AC system, and briefly introduce the way to do the impedance extraction in D-Q reference frame. The demand of impedance extraction, discussion of existing technologies, and summary for impedance measurement are also shown in this chapter.

Chapter 2 addresses the proposed algorithmic solution in detail, the algorithm of impedance calculation, Phase-Locked Loop, D-Q transform, Interpolated Fast Fourier Transform. Chapter 3 will architecture the programmed solution by MATLAB/Simulink and shows the result of the impedance model for the system from the source and load. Further apply AC/DC/AC converter to analyze the system stability.

Chapter 4 introduces the LabView FPGA design program and Multisim circuit CAD program. Architects a modified algorithm solution for impedance extraction technique. Further shows the results for the LabView and Multisim real time co-simulation.

Chapter 5 concludes and summarizes the work. Proposition for future architectural and functional improvements are made here.

## Chapter 2

### Impedance Extraction Algorithm

In this chapter, the algorithm will be shown as the solution to find the impedance model in D-Q reference frame. Both impedance measurement by perturbing voltage and currents will be introduced in this chapter. Based on the system response by these perturbations, the matrices of impedance in the D-Q frame will be calculated.

#### 2.1 Model Description

##### 2.1.1 Voltage Injected Model Description

A balanced three-phase source connected with the three-phase load is the basic circuit testing model shown in Fig 3. To make a disturbance, adding a different frequency voltage source between the source and the load in every phase. The voltage sensors should be installed between the sides of any phase of injected power source, the current sensor can be installed in before or after the injected power source. The system can be represented by the Thevenin-equivalent model in Fig 3.

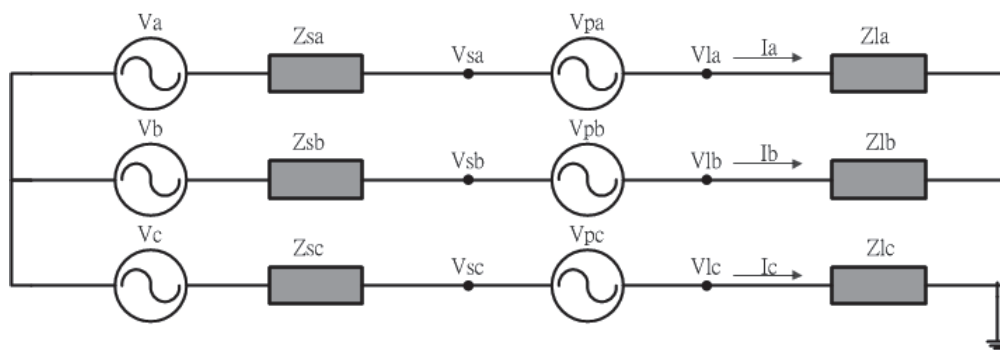


**Figure 3.** Three-Phase AC Balanced Circuit with Injected Voltages

To simplify the model, the three-phase circuit model can be seen as single-phase circuit model, the single-phase Thevenin-equivalent model can be shown as Fig 4.

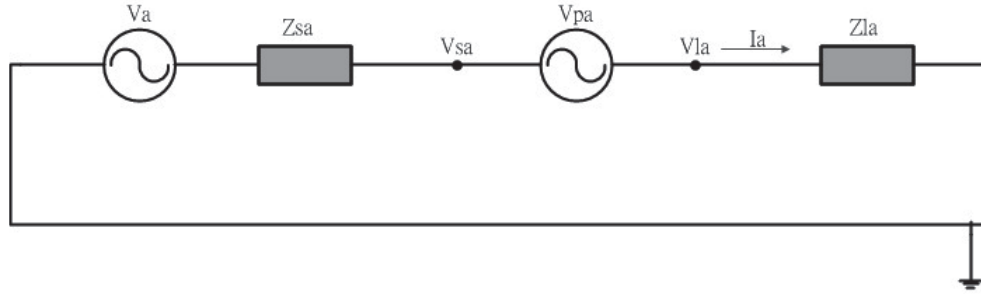


**Figure 4.** Single-Phase AC Circuit

In the single-phase system, assume  $V_a$  is in the frequency of  $w_s$  and the injected voltage is in the frequency of  $w_e$ . To apply D-Q transform, make the single phase frame as a rotating frame in the speed of  $w_s$ . Hence, the injected voltage speed will be  $w_e - w_s$ . After created an artificial frame as D-Q reference frame, the single-phase system can be seen as DC source injected by an AC voltage source with the speed of  $w_e - w_s$ , and the circuit is shown as Fig 5.

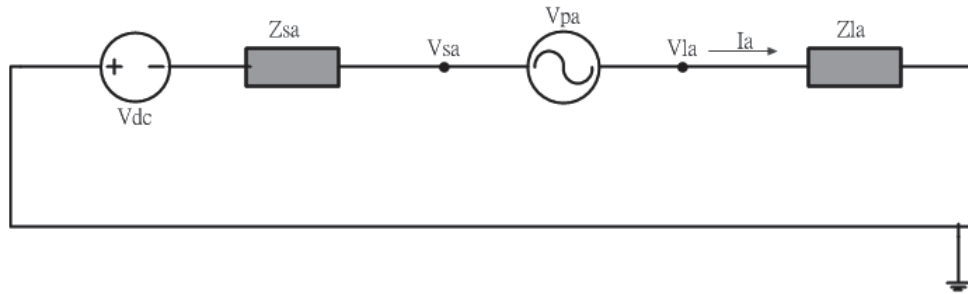


**Figure 5.** Transformed Single-Phase Circuit

To use the same concept in the three-phase system, just consider the rotate speed, the three-phase AC source in  $w_s$  and the injected source is  $w_e$ . By rotating the ABC coordinate in  $w_s$ , the AC side voltage will become DC voltage and the phase shift of each side can be ignored. The injected AC voltage will remain in the speed of  $w_e - w_s$ . The circuit is shown as Fig 6.

After using the park transformation for the three phase AC system, the equivalent system in D-Q frame will appear as follows, where  $V_d$  and  $V_q$  are constants,  $V_{pd}$  and  $V_{pq}$  are AC sinusoidal waveform as shown in Fig 7.

In the D-Q system, the  $V_d$  and  $V_q$  circuits actually are dual channel system. It means injecting voltage on D axis will also introduce voltage to Q axis. In other words, inject voltage on Q axis will also introduce voltage on V axis. So the impedance model in D-Q reference will be decoupled into two impedances model

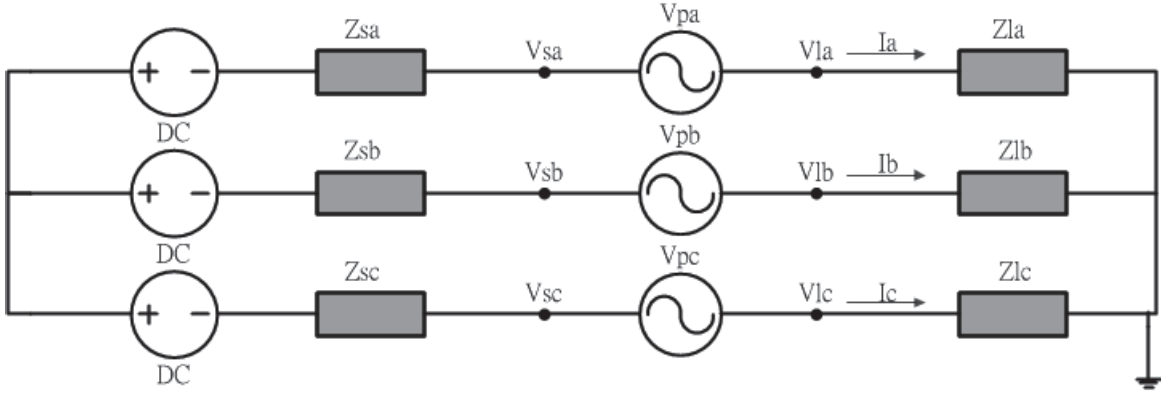


**Figure 6.** Transformed Three-Phase Circuit

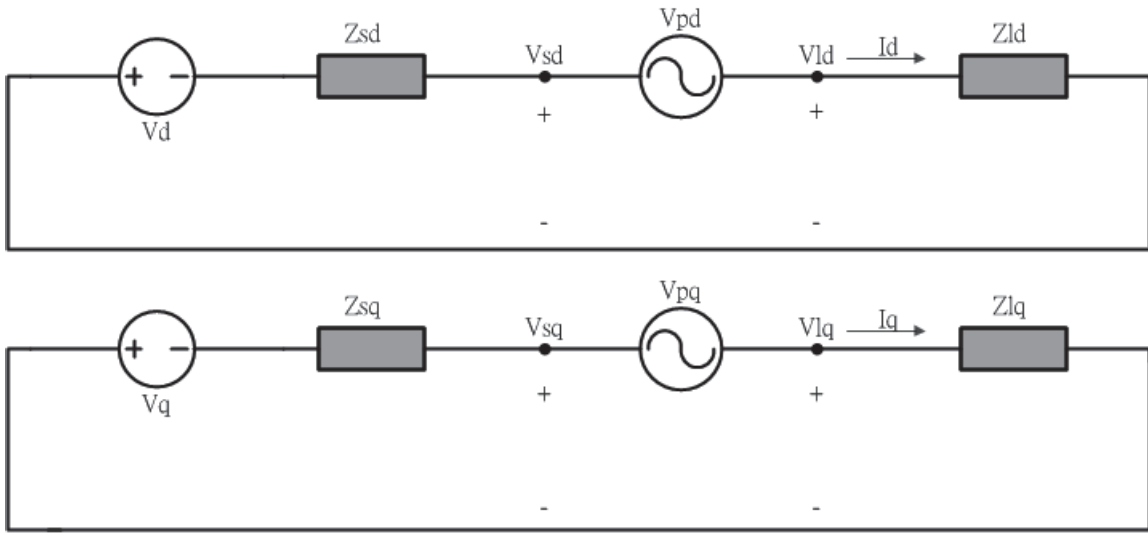


**Figure 7.** System in DQ Reference Frame

as  $Z_{dd}$ ,  $Z_{dq}$ ,  $Z_{qd}$ ,  $Z_{qq}$ . the equivalent model is shown as Fig 8. For further circuit,  $Z_{dd}$  and  $Z_{dq}$  will combine as  $Z_d$ , and  $Z_{qd}$  and  $Z_{qq}$  will combine as  $Z_q$ .

To calculate the impedance model in D-Q system, the impedance can be separated as four elements for both source and load. That means to solve the 2 by 2 matrix , the voltage injection can only produce a set of 1 by 1 matrix of voltage and a set of 1 by 1 matrix of current. The matrix can be shown as (2.1) and The equivalent circuit is shown as Fig 9.

$$\begin{bmatrix} V_{d1} \\ V_{q1} \end{bmatrix} = \begin{bmatrix} Z_{dd} & Z_{dq} \\ Z_{qd} & Z_{qq} \end{bmatrix} \times \begin{bmatrix} i_{d1} \\ i_{q1} \end{bmatrix} \quad (2.1)$$

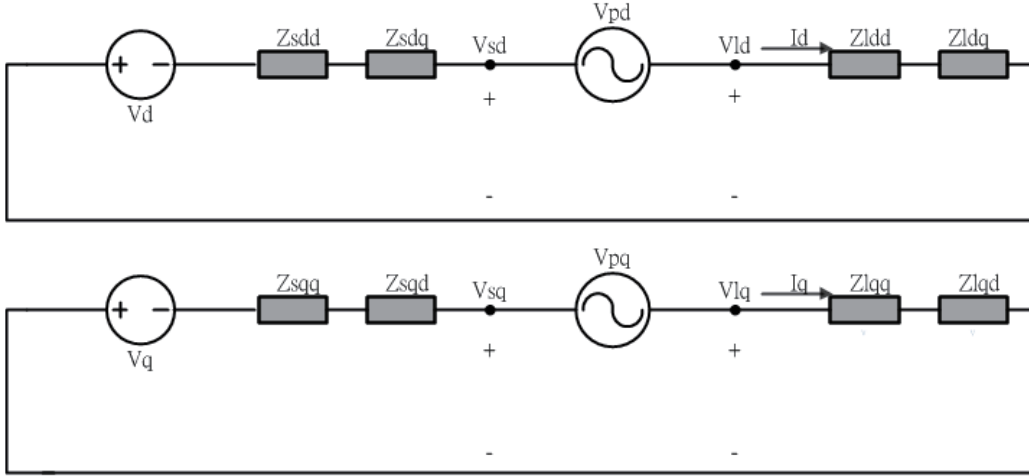


**Figure 8.** Impedance Model in DQ System

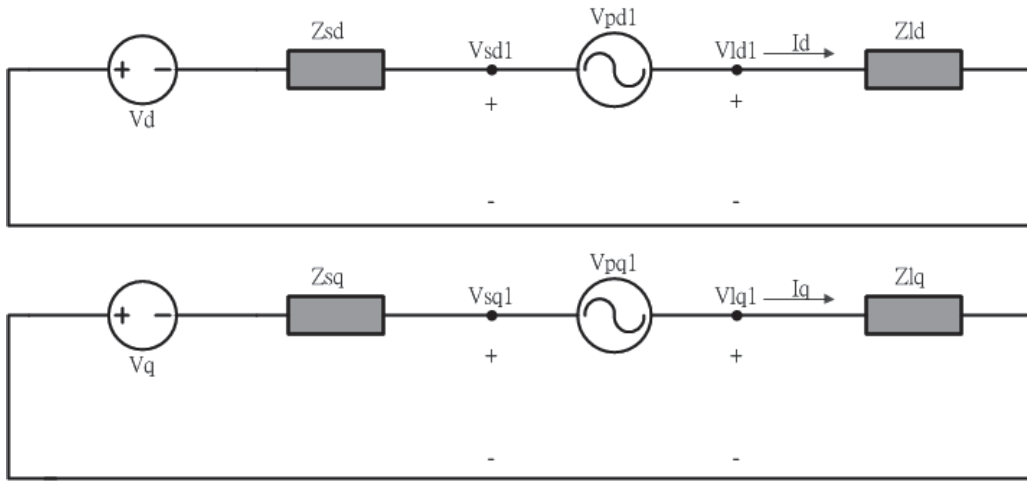


**Figure 9.** First Injection in System for DQ Reference Frame

By knowing the impedance model is a two by two matrix, the second set of voltage injection and system response are needed in order to solve the impedance matrix. Two sets of voltage injections and current responses can be combined since it is a small signal model. In consequence, the second injection voltage and current response can be written as (2.2).

$$\begin{bmatrix} V_{d2} \\ V_{q2} \end{bmatrix} = \begin{bmatrix} Z_{dd} & Z_{dq} \\ Z_{qd} & Z_{qq} \end{bmatrix} \times \begin{bmatrix} i_{d2} \\ i_{q2} \end{bmatrix} \quad (2.2)$$

Since the system is analyzed in small signal analysis, two different currents and voltages responses can do superposition, which means that two matrices can be added together. In this case, two by two matrices can be solved with simple four arithmetic operations. In order to solve the impedance model, the function of the combination of two matrices can be written as (2.3) and the second injection circuit is shown as Fig 10.

$$\begin{bmatrix} V_{d1} & V_{d2} \\ V_{q1} & V_{q2} \end{bmatrix} = \begin{bmatrix} Z_{dd} & Z_{dq} \\ Z_{qd} & Z_{qq} \end{bmatrix} \times \begin{bmatrix} i_{d1} & i_{d2} \\ i_{q1} & i_{q2} \end{bmatrix} \quad (2.3)$$

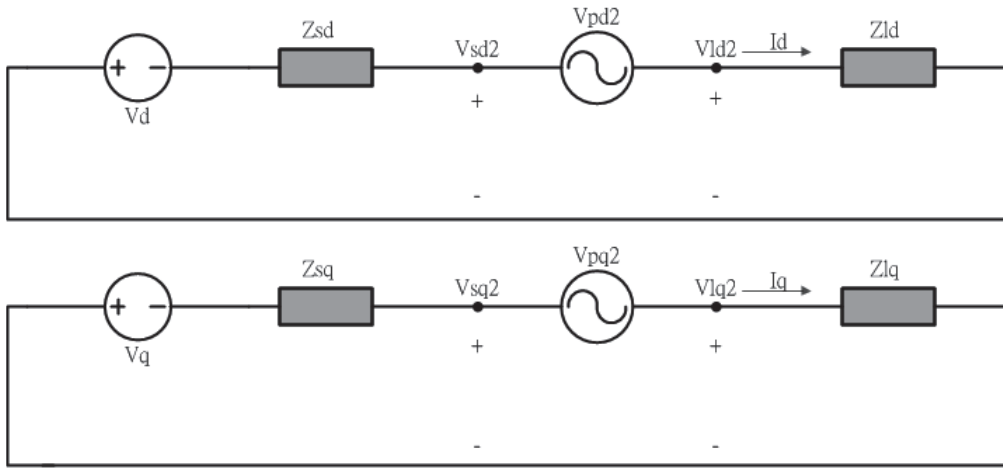


**Figure 10.** Second Injection in System for DQ Reference Frame

In the transformed D-Q reference frame system, voltages on sensors  $V_{sd}$ ,  $V_{sq}$ ,  $V_{ld}$ ,  $V_{lq}$  and currents on sensors  $I_d$  and  $I_q$  are the combination of source and disturbance source. To do the impedance extraction, to do the Fast Fourier Transformation to filter the frequency of the speed of transformed injected voltage source,  $w_e - w_s$ . The DC components can be filter out of the source, and the whole system can be changed into frequency domain with amplitude and phase angle. The circuit is shown as Fig 11.

### 2.1.2 Current Injected Model Description

A load and a source interconnected in a three-phase system can be represented as the basic circuit testing model shown in Fig 3. To make a disturbance, adding a different frequency current source from ground to the system which between the source and the load in each phase. The current sensors should install between

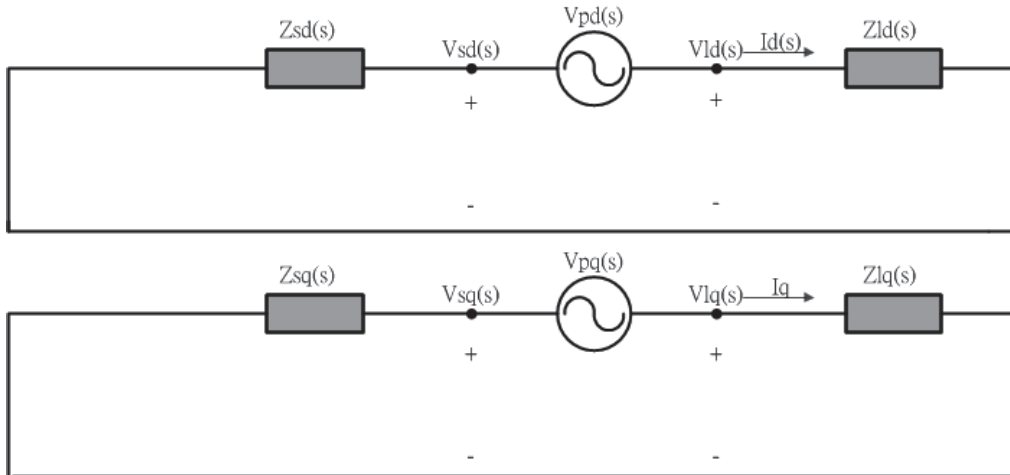


**Figure 11.** Frequency Domain for DQ Coordinate Circuit

the sides of any phase of injected power source since injected current will flow to the source side and load side, the voltage sensor can be installed in before or after the injected power source because it will maintain the same amplitude and phase angle in either part of the system. The system can be represented by the Thevenin-equivalent model in Fig 12.

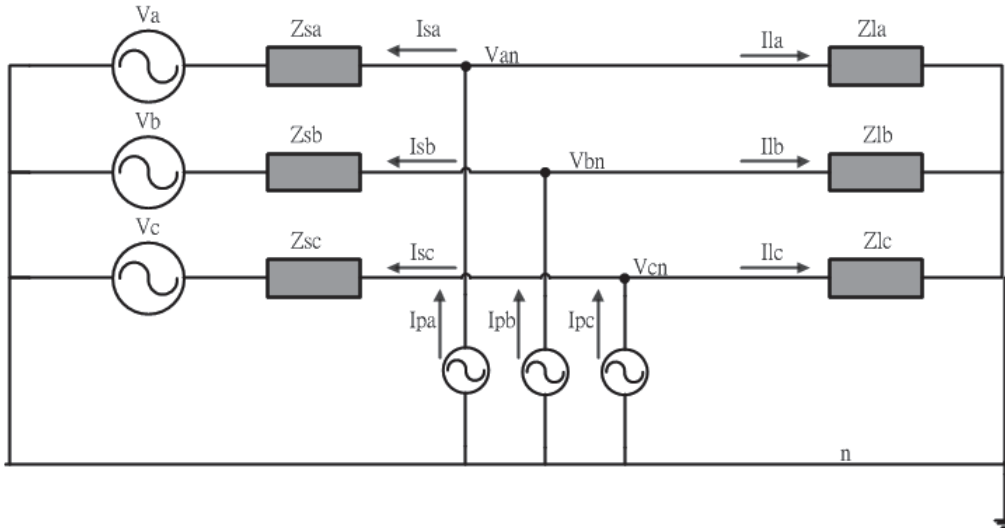


**Figure 12.** Three-Phase AC Balanced Circuit with Injected Currents

To rotate the abc coordinate as same as source speed  $w_s$ , only focus on rotate speed, the three-phase AC source in  $w_s$  and the injected source is  $w_e$ . AC side voltage will become DC voltage and the phase shift of each side can be canceled. The injected AC voltage will remain with the speed of  $w_e - w_s$ .



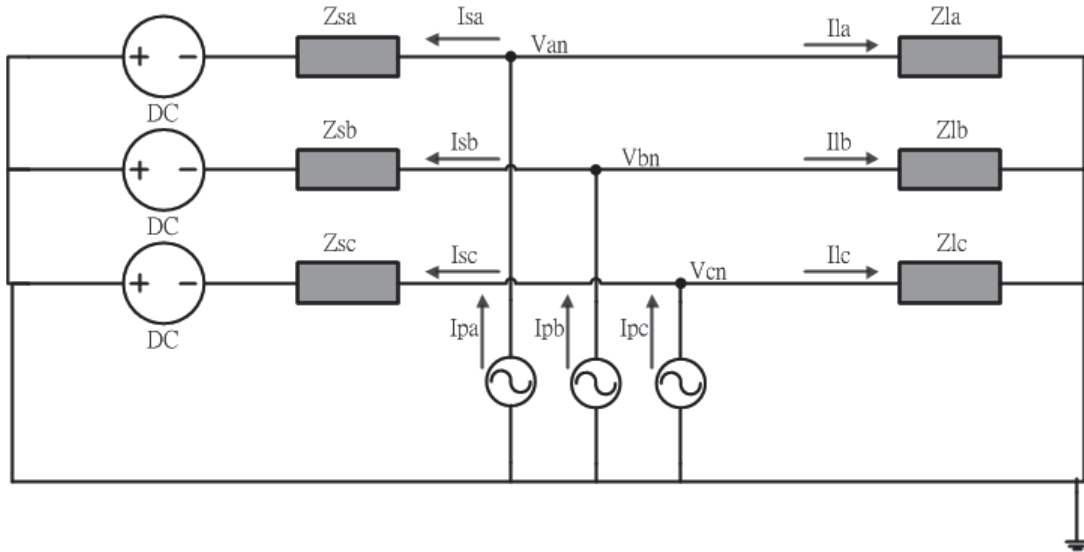


**Figure 13.** Transformed Three-Phase Circuit with Injected Currents

By applying D-Q transformation for the three-phase system, the whole system can break into D-axis and Q-axis, where  $V_d$  and  $V_q$  are constants, Injected currents  $I_{pd}$  and  $I_{pq}$ , measured voltages  $V_d$ ,  $V_q$ , and measured source currents  $I_{sd}$ ,  $I_{sq}$  and load currents  $I_{ld}$  and  $I_{lq}$  are AC component with sinusoidal waveform in the speed of  $\omega_e - \omega_s$ . The equivalent circuit is shown as Fig 14.

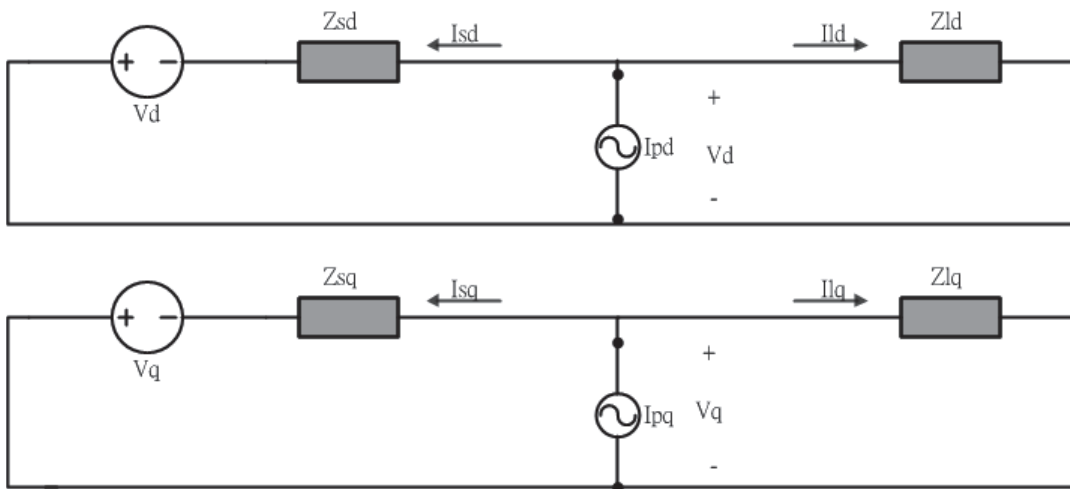


**Figure 14.** System in D-Q Coordinate

The three-phase system has been changed to double channels in D-axis and Q-axis. The two axis will be affected by each other, and they will depend on each other. So the impedance is decoupled by two

components,  $Z_{sd}$  is made by  $Z_{sdd}$  and  $Z_{sdq}$ ,  $Z_{sq}$  is composed by  $Z_{sqd}$  and  $Z_{sqq}$ ,  $Z_{ld}$  can be separated by  $Z_{ldd}$  and  $Z_{ldq}$ ,  $Z_{lq}$  can be decouple as  $Z_{lqd}$  and  $Z_{lqq}$ . The equivalent circuit can be shown as Fig 15.

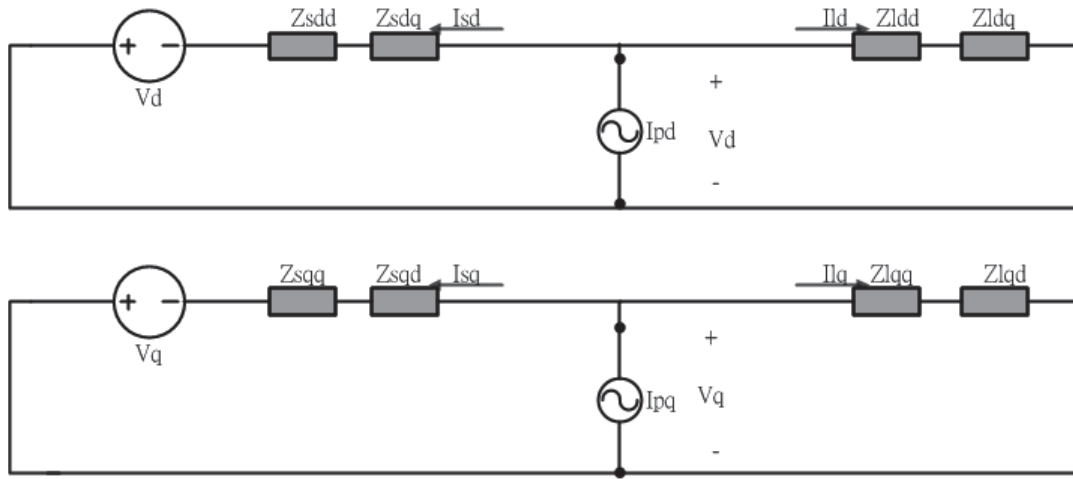


**Figure 15.** Impedance Model in D-Q Coordinate

The impedance model is a  $2 \times 2$  matrix in D-Q reference frame, the first current injection can only get one time of system response, which produces a set of source currents. In other words, the first injection can obtain two sets of  $2 \times 1$  matrix, a set of load currents and a set of voltages in both D-axis and Q-axis, the equation as mentioned previously as (2.1), and the circuit model is shown as Fig 16.

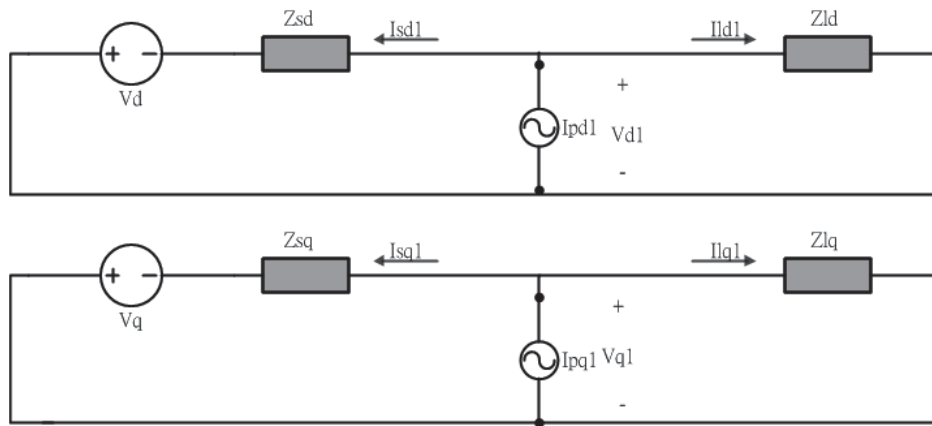


**Figure 16.** First Current Injection in DQ Reference Frame

To solve the  $2 \times 2$  impedance matrix, another set of currents and voltages is needed for solving the impedance matrix. As a consequence, the second currents injection is necessary to be injected to get second

voltage response and form (2.2), Since the system is tested and measured as small signal analysis, the two injections can be combined and the equation can be obtained as (2.3). The following circuit diagram shown as Fig 17 second injected currents.

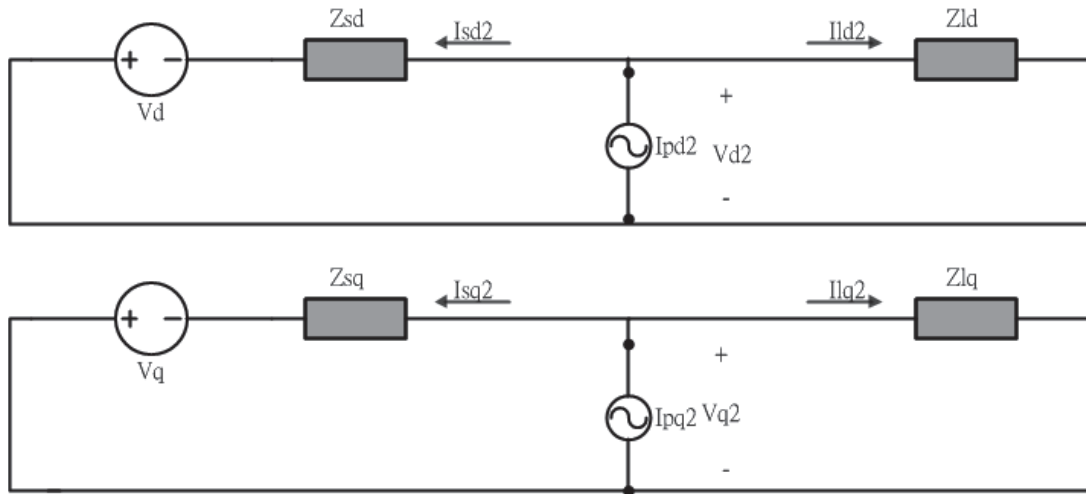


**Figure 17.** Second Current Injection in DQ Reference Frame

To find the impedance in specific frequency, the transfer function can appropriately filter unnecessary frequency components like DC component. The FFT can extract the amplitude and phase for only the AC side of disturbance. The diagram is showing below as a system in frequency domain.

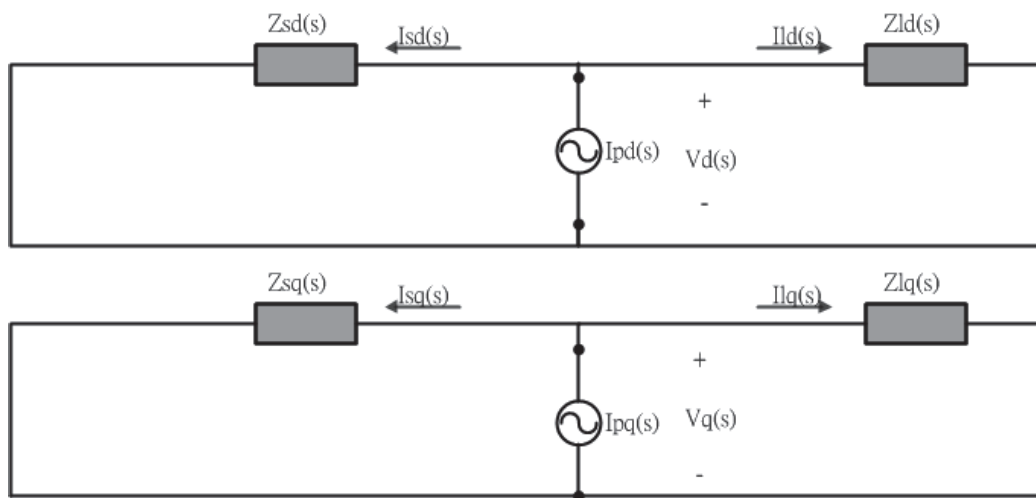


**Figure 18.** Frequency Domain in D-Q Reference Frame

## 2.2 Impedance Calculation Method

As shown in the Fig 8 and the Fig 15. A three-phase system has been changed to DC system, the artificial frame has mapped into D-axis and Q-axis. In other words, the source and load impedances are composed by four elements, each axis has two components. The source impedance and load impedance is represented as  $2 \times 2$  matrices as (2.4) and (2.5)

$$Z_{sdq} = \begin{bmatrix} Z_{sdd} & Z_{sdq} \\ Z_{sqd} & Z_{sqq} \end{bmatrix} \quad (2.4)$$

$$Z_{ldq} = \begin{bmatrix} Z_{ldd} & Z_{ldq} \\ Z_{lqd} & Z_{lqq} \end{bmatrix} \quad (2.5)$$

If all the voltages and currents can be measured directly from the system, the impedance model can be calculated by solving two sets of linear equations by superposition of two times injection. Equations are given as follows.

$$\begin{bmatrix} V_{sd1}(s) \\ V_{sq1}(s) \end{bmatrix} = \begin{bmatrix} Z_{dd}(s) & Z_{dq}(s) \\ Z_{qd}(s) & Z_{qq}(s) \end{bmatrix} \times \begin{bmatrix} i_{d1}(s) \\ i_{q1}(s) \end{bmatrix} \quad (2.6)$$

The circuit already transformed into frequency domain for extracting the impedance model in desired frequency. Fast Fourier Transform can do the effort to extract the particular frequency. Interpolated Fast Fourier Transform was used in this experiment, which will introduce in the following chapter. This equation shows the relationship between voltages and currents and it ignores the noise from the system or other external source signal.

$$\begin{bmatrix} V_{sd2}(s) \\ V_{sq2}(s) \end{bmatrix} = \begin{bmatrix} Z_{dd}(s) & Z_{dq}(s) \\ Z_{qd}(s) & Z_{qq}(s) \end{bmatrix} \times \begin{bmatrix} i_{d2}(s) \\ i_{q2}(s) \end{bmatrix} \quad (2.7)$$

A critical assumption is made by (2.1) and (2.2), the impedance does not change in the same frequency, but different injection voltage. By superposition these equations, it gives (2.8) and (2.9).

$$\begin{bmatrix} V_{sd1}(s) \\ V_{sd2}(s) \end{bmatrix} = \begin{bmatrix} i_{d1}(s) & i_{q1}(s) \\ i_{d2}(s) & i_{q2}(s) \end{bmatrix} \times \begin{bmatrix} Z_{dd}(s) \\ Z_{dq}(s) \end{bmatrix} \quad (2.8)$$

$$\begin{bmatrix} V_{sq1}(s) \\ V_{sq2}(s) \end{bmatrix} = \begin{bmatrix} i_{d1}(s) & i_{q1}(s) \\ i_{d2}(s) & i_{q2}(s) \end{bmatrix} \times \begin{bmatrix} Z_{qd}(s) \\ Z_{qq}(s) \end{bmatrix} \quad (2.9)$$

In small signal model, we can do superposition to combine (2.8) and (2.9) together, the equations can be organized as follows.

$$\begin{bmatrix} V_{sd1}(s) & V_{sq1}(s) \\ V_{sd2}(s) & V_{sq2}(s) \end{bmatrix} = \begin{bmatrix} i_{d1}(s) & i_{q1}(s) \\ i_{d2}(s) & i_{q2}(s) \end{bmatrix} \times \begin{bmatrix} Z_{dd}(s) & Z_{dq}(s) \\ Z_{qd}(s) & Z_{qq}(s) \end{bmatrix} \quad (2.10)$$

Finally, the  $2 \times 2$  impedance matrix can be solve when voltages and currents are in the same dimension. Multiplying the inverse current matrix to voltage gives the impedance model shown as (2.11), two elements on each axis.

$$\begin{bmatrix} Z_{dd}(s) & Z_{dq}(s) \\ Z_{qd}(s) & Z_{qq}(s) \end{bmatrix} = \begin{bmatrix} V_{sd1}(s) & V_{sq1}(s) \\ V_{sd2}(s) & V_{sq2}(s) \end{bmatrix} \times \begin{bmatrix} i_{d1}(s) & i_{q1}(s) \\ i_{d2}(s) & i_{q2}(s) \end{bmatrix}^{-1} \quad (2.11)$$

### 2.2.1 Injection Restriction

There are a couple of impedance limitations for the test model. For instance, current injects into the middle of a system, injected currents will flow to both source side and load side. The voltage is equal to the source currents multiply by source impedance, also equal to load currents multiply by load impedance. All in all, under current injection, voltage will stay the same no matter in source side of system or load side of system. Voltage in D-axis are made by current in D-axis and impedance on both axes. Voltage in Q-axis are made by current in Q-axis and impedance on both axes. To express in matrix, impedance model is a two by two matrix. The equation for the source subsystem is (2.12).

$$\begin{bmatrix} V_d(s) \\ V_q(s) \end{bmatrix} = \begin{bmatrix} Z_{sdd}(s) & Z_{sdq}(s) \\ Z_{sqd}(s) & Z_{sqq}(s) \end{bmatrix} \begin{bmatrix} i_{sd}(s) \\ i_{sq}(s) \end{bmatrix} \quad (2.12)$$

$$\begin{bmatrix} V_d(s) \\ V_q(s) \end{bmatrix} = \begin{bmatrix} Z_{ldd}(s) & Z_{ldq}(s) \\ Z_{lqd}(s) & Z_{lqq}(s) \end{bmatrix} \begin{bmatrix} i_{ld}(s) \\ i_{lq}(s) \end{bmatrix} \quad (2.13)$$

Next, the load side of the system has large amount of similarity compare to the source side. However, even though inject same voltage into the system, load current responses are different compare to source current response. In consequence, load impedance is different between source impedance.

Voltages stay the same in two sides of source and load, which means the voltages of (2.12) is equal to the voltages of (2.13).

$$\begin{bmatrix} Z_{sdd}(s) & Z_{sdq}(s) \\ Z_{sqd}(s) & Z_{sqq}(s) \end{bmatrix} \begin{bmatrix} i_{sd}(s) \\ i_{sq}(s) \end{bmatrix} = \begin{bmatrix} Z_{ldd}(s) & Z_{ldq}(s) \\ Z_{lqd}(s) & Z_{lqq}(s) \end{bmatrix} \begin{bmatrix} i_{ld}(s) \\ i_{lq}(s) \end{bmatrix} \quad (2.14)$$

By the circuit theory, the nodal equation at the point of common coupling becomes the following.

$$\begin{bmatrix} I_{pd}(s) \\ I_{pq}(s) \end{bmatrix} = \begin{bmatrix} I_{sd}(s) \\ I_{sq}(s) \end{bmatrix} + \begin{bmatrix} i_{ld}(s) \\ i_{lq}(s) \end{bmatrix} \quad (2.15)$$

Substituting source current and load current gives.

$$\begin{bmatrix} I_{pd}(s) \\ I_{pq}(s) \end{bmatrix} = \begin{bmatrix} Z_{sdd}(s) & Z_{sdq}(s) \\ Z_{sqd}(s) & Z_{sqq}(s) \end{bmatrix}^{-1} \begin{bmatrix} V_d(s) \\ V_q(s) \end{bmatrix} + \begin{bmatrix} Z_{ldd}(s) & Z_{ldq}(s) \\ Z_{lqd}(s) & Z_{lqq}(s) \end{bmatrix}^{-1} \begin{bmatrix} V_d(s) \\ V_q(s) \end{bmatrix} \quad (2.16)$$

Organizing (2.16) and extracting voltages out, which gives.

$$\begin{bmatrix} V_d(s) \\ V_q(s) \end{bmatrix} = \left[ \begin{bmatrix} Z_{sdd}(s) & Z_{sdq}(s) \\ Z_{sqd}(s) & Z_{sqq}(s) \end{bmatrix}^{-1} + \begin{bmatrix} Z_{ldd}(s) & Z_{ldq}(s) \\ Z_{lqd}(s) & Z_{lqq}(s) \end{bmatrix}^{-1} \right]^{-1} \begin{bmatrix} I_{pd}(s) \\ I_{pq}(s) \end{bmatrix} \quad (2.17)$$

It can be observed that if one side of impedance model is critically small, voltages become hard to perturbation by the injected currents. Voltages can be substituted by load currents and load impedance. Modifying Eq. (2.17) which gives. (2.18) can do the further organize as (2.19).

$$\begin{aligned} & \left[ \begin{bmatrix} Z_{sdd}(s) & Z_{sdq}(s) \\ Z_{sqd}(s) & Z_{sqq}(s) \end{bmatrix}^{-1} + \begin{bmatrix} Z_{ldd}(s) & Z_{ldq}(s) \\ Z_{lqd}(s) & Z_{lqq}(s) \end{bmatrix}^{-1} \right]^{-1} \begin{bmatrix} I_{pd}(s) \\ I_{pq}(s) \end{bmatrix} \\ & = \begin{bmatrix} I_{ld}(s) \\ I_{lq}(s) \end{bmatrix} \begin{bmatrix} Z_{ldd}(s) & Z_{ldq}(s) \\ Z_{lqd}(s) & Z_{lqq}(s) \end{bmatrix} \end{aligned} \quad (2.18)$$

$$\begin{aligned}
& \begin{bmatrix} Z_{ldd}(s) & Z_{ldq}(s) \\ Z_{lqd}(s) & Z_{lqq}(s) \end{bmatrix}^{-1} \begin{bmatrix} Z_{sdd}(s) & Z_{sdq}(s) \\ Z_{sqd}(s) & Z_{sqq}(s) \end{bmatrix}^{-1} + \begin{bmatrix} Z_{ldd}(s) & Z_{ldq}(s) \\ Z_{lqd}(s) & Z_{lqq}(s) \end{bmatrix}^{-1} \begin{bmatrix} I_{pd}(s) \\ I_{pq}(s) \end{bmatrix} \\
& \hspace{20em} = \begin{bmatrix} I_{ld}(s) \\ I_{lq}(s) \end{bmatrix}
\end{aligned} \tag{2.19}$$

## 2.3 Injection Concept

### 2.3.1 Injected Voltage Selection

To solve the matrix, the premise is that these two equations should be linear independent. The equations can not be solved if they are proportional or two equations are parallel. The two different injections should choose deliberately in order to create two linear independent equations. Consider a pure sinusoidal balanced three phase voltage source system without any signal or external effect. The three-phase voltage equation is shown as (2.20).

$$\begin{aligned}
V_a &= V_m \cos(w_s t) \\
V_b &= V_m \cos(w_s t - 2\pi/3) \\
V_c &= V_m \cos(w_s t + 2\pi/3)
\end{aligned} \tag{2.20}$$

The injected voltage can be simple sinusoidal waveform with the frequency. The frequency should be the same as source frequency  $w_s$  plus measured frequency  $w_e$ . The amplitude of injected voltages is much less than the amplitude of source voltages but can still produce disturbance. The three phase injected voltage can be shown as (2.21).

$$\begin{aligned}
V_{pa} &= V_n \cos(w_s t + w_e t) \\
V_{pb} &= V_n \cos(w_s t + w_e t - 2\pi/3) \\
V_{pc} &= V_n \cos(w_s t + w_e t + 2\pi/3)
\end{aligned} \tag{2.21}$$

The park transform equation which ignored 0-axis is shown as (2.22). The reason to ignore the 0-axis is the thesis focusing on balanced systems. If the system is balanced, the 0-axis always stays zero since the park transform will cancel each phase. Multiplying (2.21) and (2.22) to obtain the d-axis and q-axis volt-

ages. Since the abc coordinate to d-q coordinate with the frequency of  $w_s$ , the injected voltage left frequency only in  $w_e$ , which is shown in (2.23).

$$\begin{bmatrix} V_d \\ V_q \end{bmatrix} = 2/3 \begin{bmatrix} \cos(w_s t) & \cos(w_s t - 2\pi/3) & \cos(w_s t + 2\pi/3) \\ \sin(w_s t) & \sin(w_s t - 2\pi/3) & \sin(w_s t + 2\pi/3) \end{bmatrix} \begin{bmatrix} V_a \\ V_b \\ V_c \end{bmatrix} \quad (2.22)$$

$$\begin{aligned} V_{dinj1} &= 1/\sqrt{3}V_n \cos(w_e t) + \dots \\ V_{qinj1} &= 1/\sqrt{3}V_n \sin(w_e t) + \dots \end{aligned} \quad (2.23)$$

For second injection, the second voltage and first voltage should be linear dependent. Select the voltage with speed that is frequency  $w_s$  minus measured frequency  $w_e$ . The second voltage injection equation is shown as (2.24). Multiplying both (2.22) and (2.24) can obtain the following equation (2.25), which can be rewritten as (2.26).

$$\begin{aligned} V_{pa} &= V_n \cos(w_s t - w_e t) \\ V_{pb} &= V_n \cos(w_s t - w_e t - 2\pi/3) \\ V_{pc} &= V_n \cos(w_s t - w_e t + 2\pi/3) \end{aligned} \quad (2.24)$$

$$\begin{aligned} V_{dinj2} &= 1/\sqrt{3}V_n \cos(-w_e t) + \dots \\ V_{qinj2} &= 1/\sqrt{3}V_n \sin(-w_e t) + \dots \end{aligned} \quad (2.25)$$

$$\begin{aligned} V_{dinj2} &= 1/\sqrt{3}V_n \cos(w_e t) + \dots \\ V_{qinj2} &= -1/\sqrt{3}V_n \sin(w_e t) + \dots \end{aligned} \quad (2.26)$$

By choosing these two voltage injection, d-axis voltages are symmetrical with same magnitude and phase. Q-axis voltages are symmetrical with same magnitude but opposite phase. Based on the concept, two voltages are not directly proportional which means they are linearly independent. The Fig 20 can clearly shown two selected voltage vectors in the D-Q reference frame.



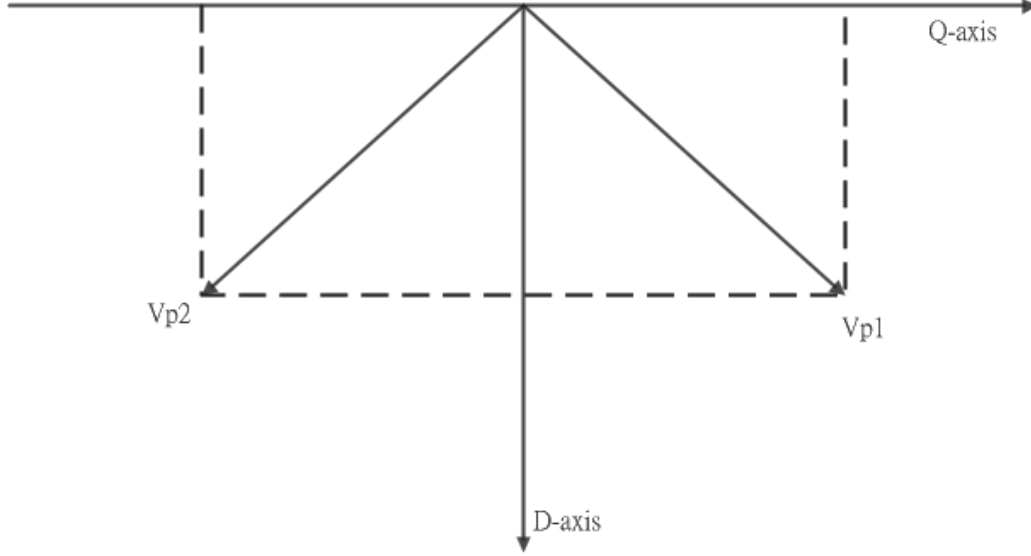


**Figure 19.** Vector Diagram of Injected Voltages in D-Q Frame

### 2.3.2 Injected Current Selection

The same concept can also apply to the current injection, the current source can be described in sinusoidal waveform with the following equation.

$$\begin{aligned}
 I_a &= I_m \cos(\omega_s t) \\
 I_b &= I_m \cos(\omega_s t - 2\pi/3) \\
 I_c &= I_m \cos(\omega_s t + 2\pi/3)
 \end{aligned} \tag{2.27}$$

First three-phase balanced current injection can pick with an appropriate magnitude and the speed of source frequency  $\omega_s$  and measured frequency  $\omega_e$ , Eq. (2.28) represents the injection currents.

$$\begin{aligned}
 I_{pa} &= I_n \cos(\omega_s t + \omega_e t) \\
 I_{pb} &= I_n \cos(\omega_s t + \omega_e t - 2\pi/3) \\
 I_{pc} &= I_n \cos(\omega_s t + \omega_e t + 2\pi/3)
 \end{aligned} \tag{2.28}$$

Second current injection can pick the same magnitude as the first injection, but different frequency compare to the first injection. The frequency should choose as frequency  $\omega_s$  minus measured frequency  $\omega_e$ . If  $\omega_e$  is bigger than  $\omega_s$ , the system can not produce negative frequency in the real world. As a consequence,

the injection can be changed from positive sequence to negative sequence because the negative sequence has the same effect as negative frequency.

$$\begin{aligned}
 I_{pa} &= I_n \cos(w_s t - w_e t) \\
 I_{pb} &= I_n \cos(w_s t - w_e t - 2\pi/3) \\
 I_{pc} &= I_n \cos(w_s t - w_e t + 2\pi/3)
 \end{aligned} \tag{2.29}$$

The D-Q axis currents has been obtained by separately multiplying (2.22), (2.28), and (2.29). All Injected currents in D-Q coordinate can be expressed as.

$$\begin{aligned}
 I_{dinj1} &= 1/\sqrt{3}V_n \cos(w_e t) + \dots \\
 I_{qinj1} &= 1/\sqrt{3}V_n \sin(w_e t) + \dots \\
 \text{and} & \\
 I_{dinj2} &= 1/\sqrt{3}V_n \cos(w_e t) + \dots \\
 I_{qinj2} &= -1/\sqrt{3}V_n \sin(w_e t) + \dots
 \end{aligned} \tag{2.30}$$

By using the same concept as voltage inject selection, two current injections are linear independent which means  $2 \times 2$  impedance matrix can be solved by those injections and responses.

Above shows appropriate disturbances for both current injection and voltage disturbance to form two linear independent function to solve the impedance matrix. The concept of impedance extraction and algorithm also are introduced in detail in this chapter. In chapter 3, the paper will introduce the algorithm architect with software simulation program in MATLAB, Simulink and Simpower.

## Chapter 3

### MATLAB Algorithm Architect

After assuming the impedance extraction can be solved by the algorithm mentioned above, the simulation model can be built to implement the technique. This chapter will introduce the programming algorithm by using MATLAB, Simulink and Simpower to cooperate with each other. A simple RL circuit with voltage perturbation will be built by Simpower with reasonable parameters for the impedance and voltage sources and voltage injection. Later on, the Phase-Locked Loop will be introduced in order to implement park transform. Interpolated Fast Fourier Transformation will be used to obtain more accurate amplitudes and phase shift. Finally, the impedance extraction technique will apply on AC/DC/AC converter circuit system to test the system stability.

#### 3.1 Model Description and Parameters

Using voltage injection to a simple RL circuit drawn by the Simpower, in this circuit, a three-phase fixed  $60Hz$  frequency voltage source feeds to the R-L load with small impedance as a bus impedance. The voltage sensors put on both sides of voltage injection to directly measure the voltage, the current sensor installed between the source side and perturbation. Voltage source and injected voltage source are all three-phase balanced voltage source. The injected Voltage source is ideal controllable since the voltage frequency should be changed during a period of time. The parameter of the whole system is shown in table 1.

The source voltage is a balanced three-phase system, with peak voltage is  $375\text{ V}$  in  $60Hz$  and the graph as Fig 21. Ideal voltage controlled source with peak voltage in 4 volts. Take test frequency  $w_e$  as  $100Hz$ , so the first voltage injection will in the speed of  $60Hz + 100Hz$ . The second injection happens in 2.5 second with  $w_s - w_e$  which is  $60Hz - 100Hz$ . However, the voltage can't create minus frequency. Hence, reverse the phase sequence to reach the negative frequency which shows in Fig 22.

The voltage measured on the load shown in Fig 23 can be observed two types of waveform combined together, although it is not very clear since the disturbance magnitude is relatively much smaller than the source voltage.

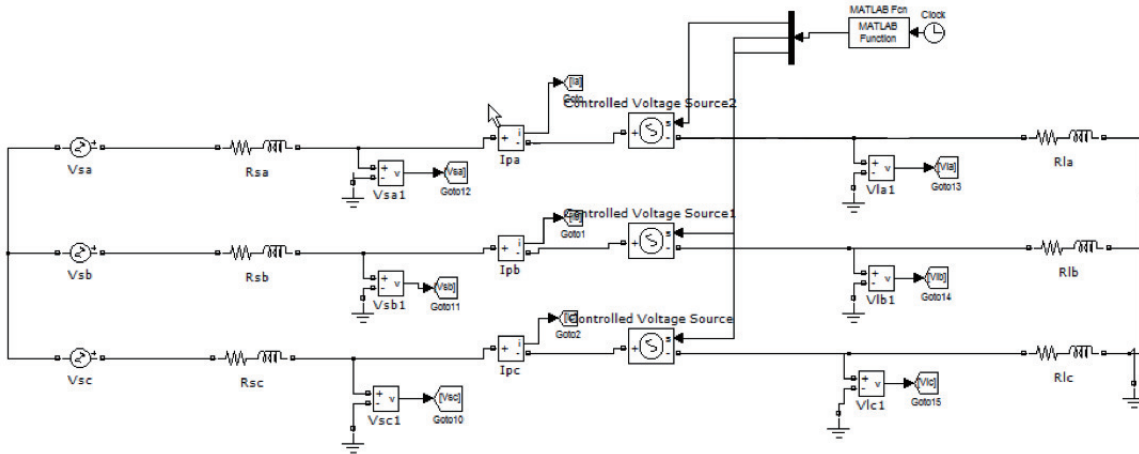


**Figure 20.** Simulation RL Circuit in Simpower

**Table 1** Simple Circuit Parameters

Peak source voltages(per phase)	376V
Peak injection voltages(per phase)	4 V
Source resistance	$0.01\Omega$
Source inductance	$10\mu H$
Load resistance	$7\Omega$
Load inductance	$460\mu H$
Testing Frequency Range	$1Hz - 10kHz$

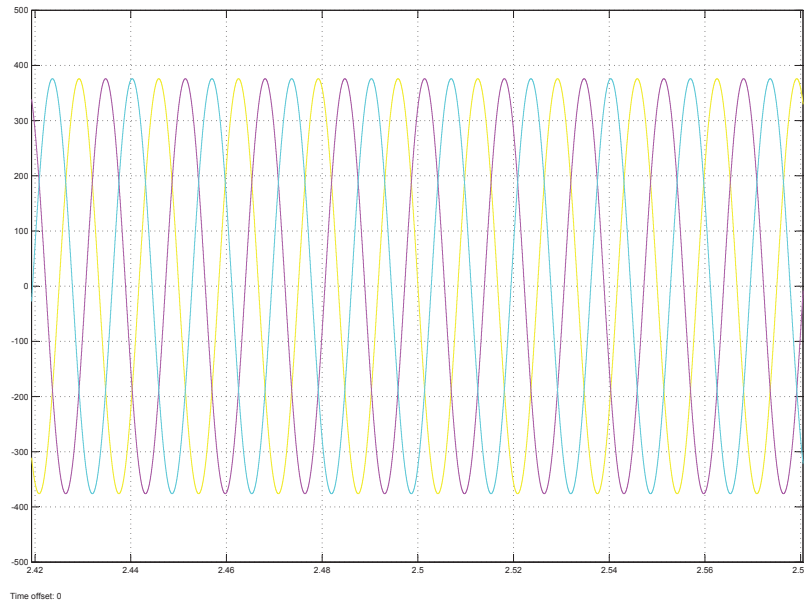


**Figure 21.** Source Voltage Scope in Simulink

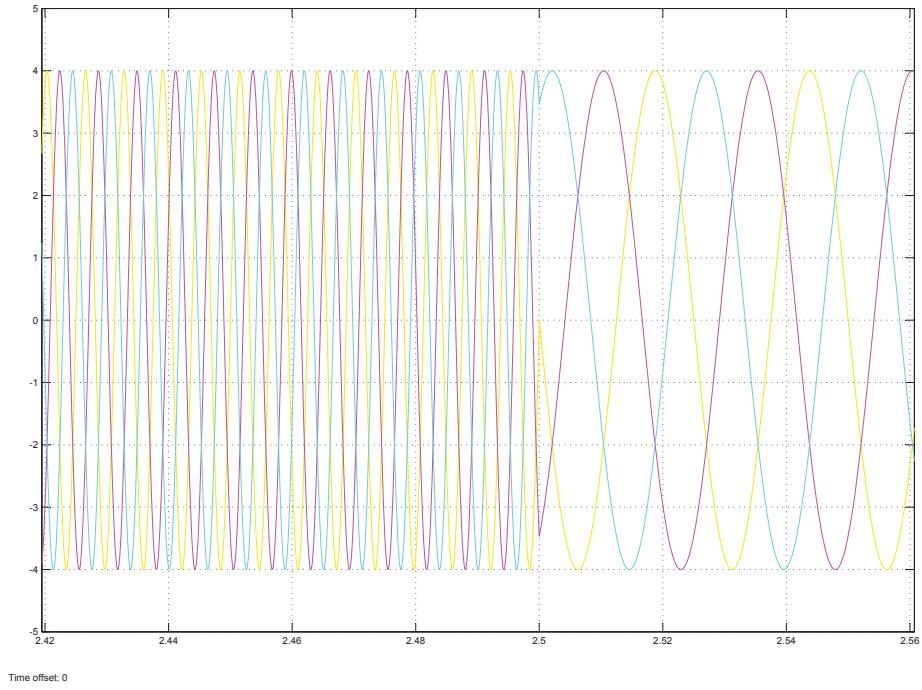


**Figure 22.** Ideal Voltage Controlled Source

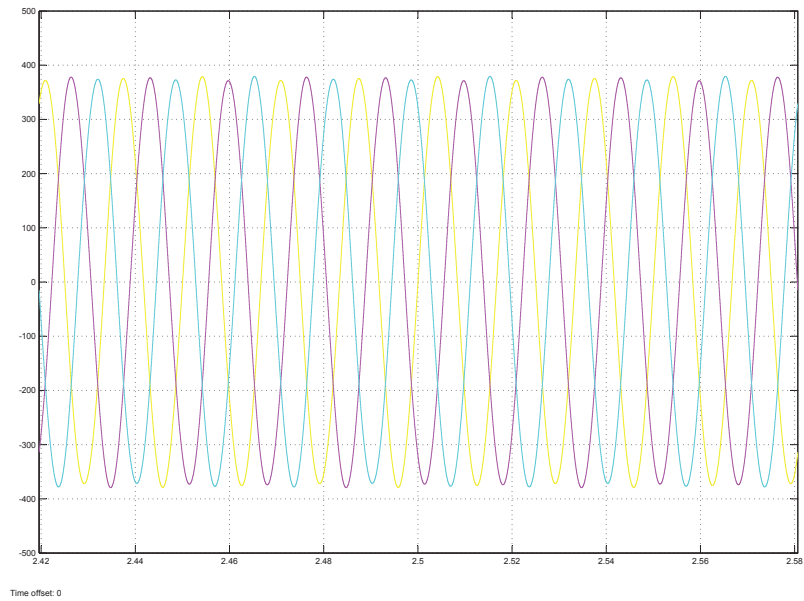


**Figure 23.** Load Voltage Scope in Simulink

### 3.2 Phase-Locked Loop

In the D-Q reference frame of the system, the impedance is composed by  $Z_{dd}$ ,  $Z_{dq}$ ,  $Z_{qd}$ ,  $Z_{qq}$ . If the coordinate is not rotate steady, the system will produce different D-axis and Q-axis which will lead to different impedance model. As a consequence, this paper align all D-axis with voltage vector, so Q-axis is 90 degree delay the D-axis close to zero. The principle of Phase-Locked Loop is showing as Fig 24.

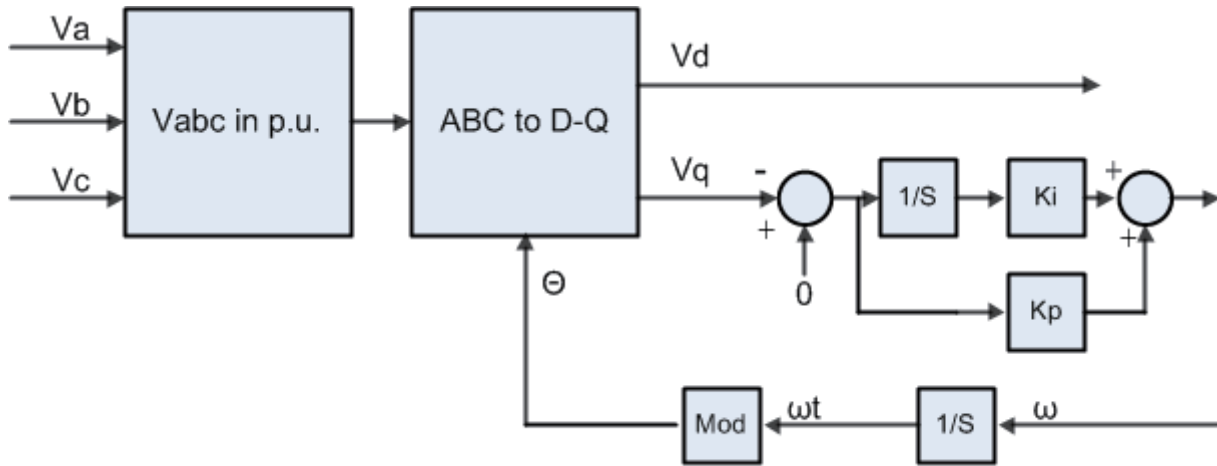


**Figure 24.** Block Diagram of Phase-Locked Loop

#### 3.2.1 Design Principle and Effects

The Phase-Locked Loop is designed as following steps. First, collect the data waveform from the source  $V_a$ ,  $V_b$  and  $V_c$  and convert them into p.u. for accurate calculation. Then, transform them to D-Q reference frame with park transformation and a reference angle  $\theta$ . The  $V_q$  should close to zero as the report mentioned in the beginning of this chapter, so the reference  $V_{qr}$  should give as zero to compare the real calculated  $V_q$  to estimate the error to do the closed loop control. If the PLL frequency is close to the line frequency and if  $V_q$  is positive, then the reference frame is behind the actual voltage vector. Then,  $V_q$  will reach to zero by increasing the reference frame speed. On the contrary, if  $V_q$  is negative, then the reference is leading the actual voltage vector. The reference speed can be decreased to adjust  $V_q$  to zero. To trace the system frequency, phase-locked loop should be locked in the same frequency as the system without little error. For instance, if the system is  $60Hz$  and the PLL is locked in the  $59Hz$ , Voltage in DQ domain will both have  $1Hz$  harmonic which makes the system in an unstable stage. To accomplished the tracing task. A PI controller is necessary for PLL. A PI controller can reduce the noticeable effect on the PLL estimated

frequency and actual frequency. The equation for PI control is showing as (3.1). The  $k_p$  is parameter for proportional gain and  $k_i$  is parameter for integral gain

$$w = k_p V_q + k_i \int V_q dt \quad (3.1)$$

By observing the equation (3.1), it shows that the integral gain  $k_i$  cannot be changed in a short period, by moving the integral gain  $k_i$  to the integral term, the  $K_i$  can be changed suddenly. The equation (3.2) organizes the PI control equation (3.1) which moves the integral gain into integral term.

$$w = k_p V_q + \int k_i V_q dt \quad (3.2)$$

By using (3.2), the  $V_q$  can be very small and the system speed  $w$  can be traced accurately without harmonic. The following block diagram is the PLL design by MATLAB/Simulink as Fig 25.

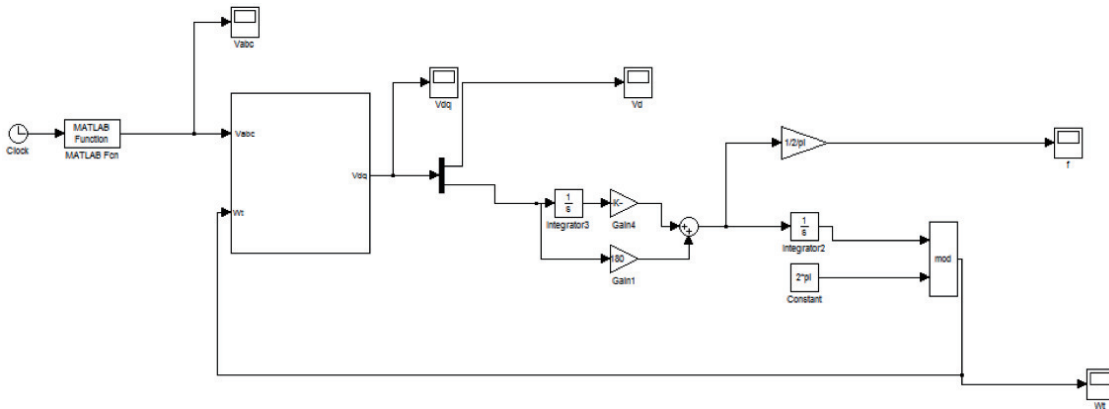


**Figure 25.** Phase-Locked Loop Design in MATLAB/Simulink

### 3.2.2 PLL Designed by MATLAB/Simulink

An important consideration is that for the reference angle produced by PI controller is  $w$ . The speed should be further convert to a variable change with time. Hence, after signal passing the PI controller, integral the signal as  $wt$  and modulus by  $2\pi$  to produce ramp signal with angle range from 0 degree to 360 degree in radians. The ramp signal is shown as Fig 26.

The following figure shows the park transformation from ABC coordinate to D-Q reference frame as two DC components with Q-axis as 0 and D-axis with the voltage vector as source voltage.

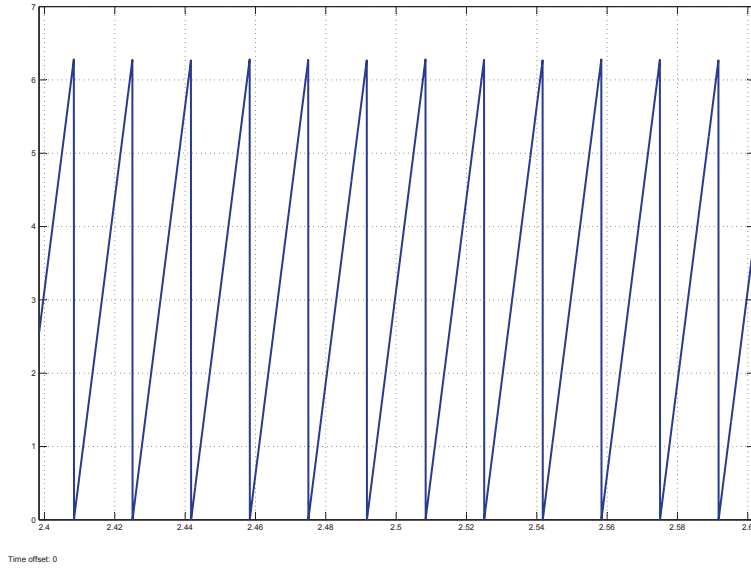


**Figure 26.** Ramp Signal By MATLAB/Simulink

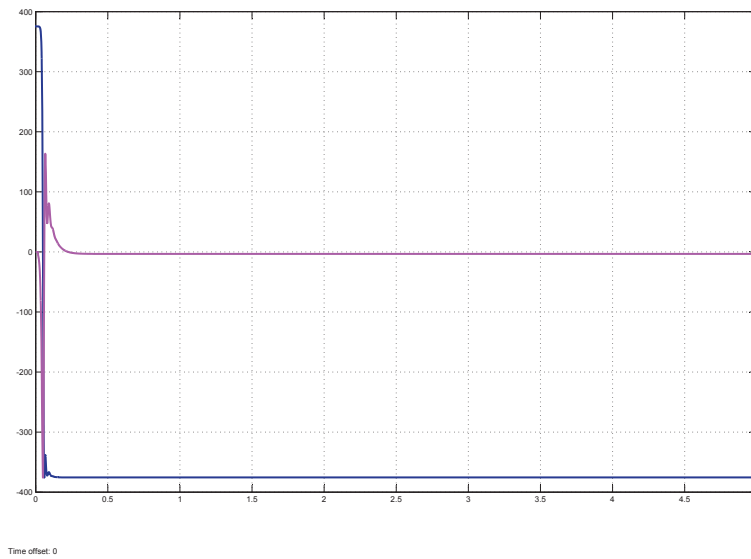


**Figure 27.** Source Voltage Transformed in DQ Reference Frame



### 3.3 DQ Transform With Voltage Perturbation

After Successfully implementing DQ transform with PLL and PI controller, another voltage source with other frequency will be injected to produce perturbation. Since the perturbation added with different frequency from the source. It can be seen as two different waveform combine with each other. By doing DQ transform based on source frequency. The perturbation voltage will cause sinusoidal fluctuations.

The injected frequency is source frequency plus test frequency  $w_s + w_e$ , after DQ transform locked with source frequency, the perturbation frequency after DQ transformation will be  $w_s + w_e - w_s$  equal to  $w_e$ . Take test frequency  $160Hz$  and source frequency  $60Hz$  as an example. Injected voltage source after DQ transform will be  $160Hz - 60Hz$  is  $100Hz$ . Fig 28 shows the sinusoidal fluctuation in DQ reference frame.

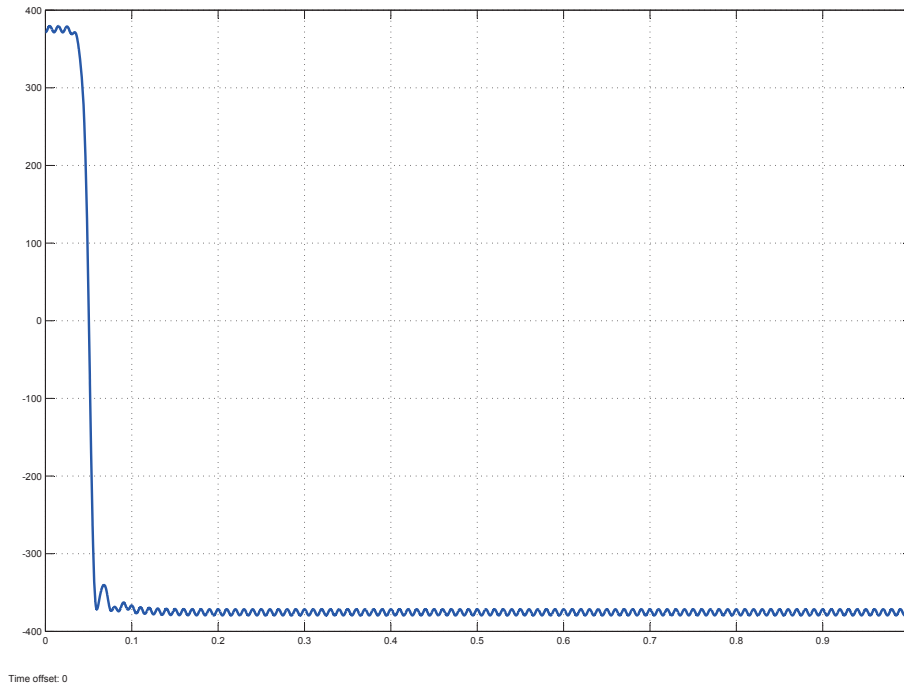


**Figure 28.** Sinusoidal Fluctuation in D-Axis

In the diagrams showing from Fig 28 to Fig 31, the perturbation is clearly shown. Voltage with  $160Hz$  frequency and reasonable magnitude injected into a system to cause the perturbation. DQ transform algorithm by doing signal processing. The DQ reference frame has both perturbations with  $100Hz$  frequency. Figures f show the disturbance in stable state after 0.5 seconds.

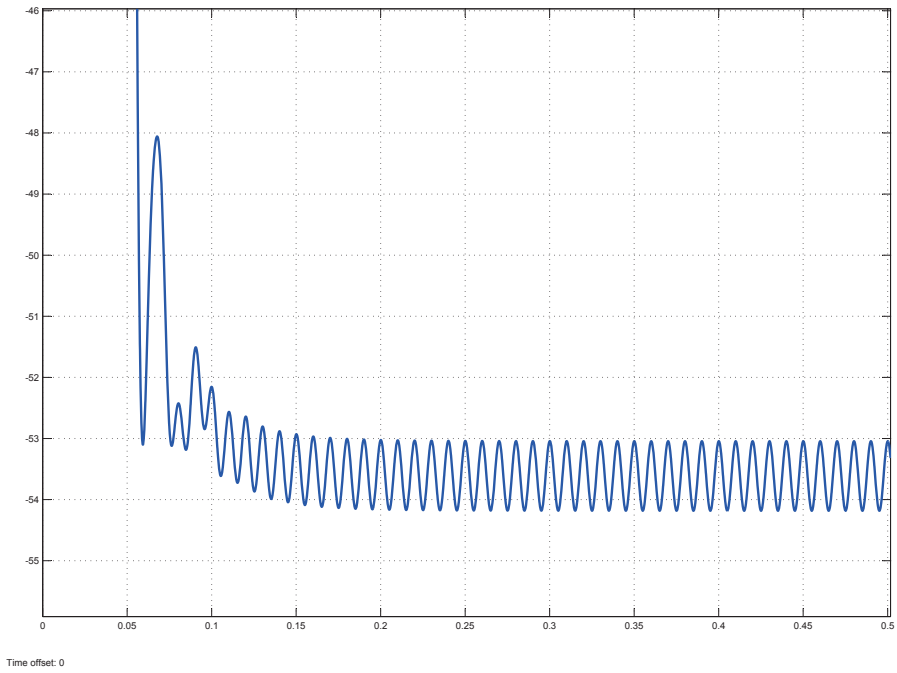


**Figure 29.** Clear Sinusoidal Fluctuation in D-Axis

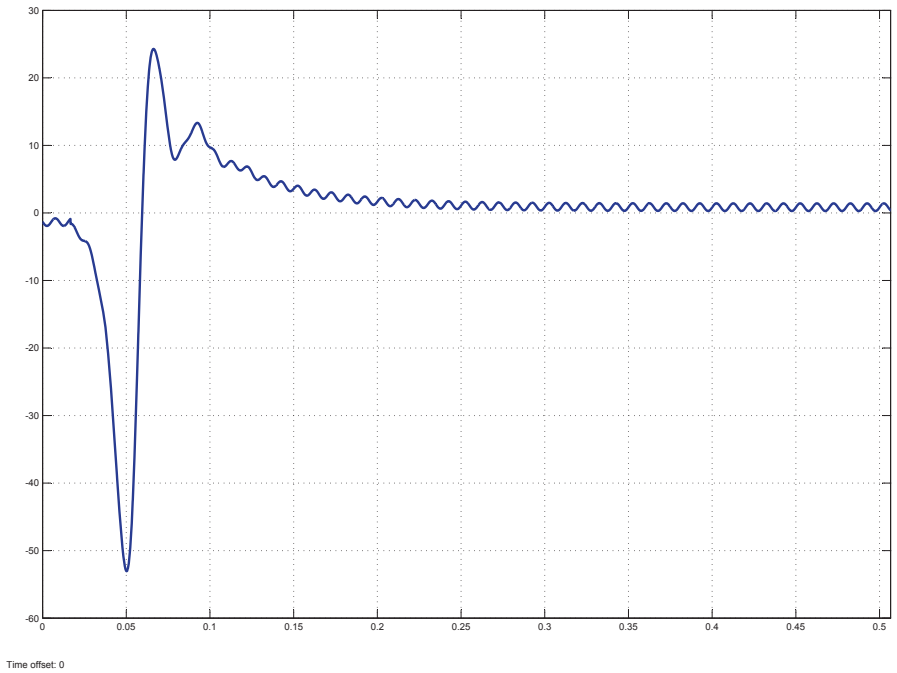


**Figure 30.** Sinusoidal Fluctuation in Q-Axis

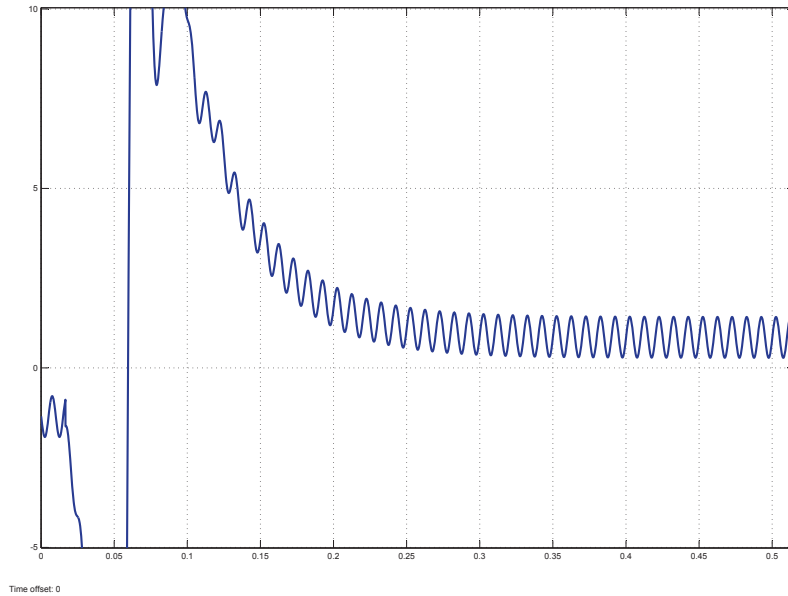


**Figure 31.** Clear Sinusoidal Fluctuation in Q-Axis

### 3.4 Interpolated Fast Fourier Transformation

The Fast Fourier Transformation can be treated as a filter. In DQ coordinates, the signal is composed by DC component and sinusoidal waveform. The sinusoidal waveform is the target waveform to do the impedance extraction. Hence, FFT can be applied in order to extract target waveform to do the further calculation. Since, the experiment is doing the frequency from  $1Hz$  to  $10kHz$ , the experiment time will stay long and separated with many segments. Interpolated Fast Fourier Transform [14] is designed to deal with several segments and also extract the magnitude and phase angle for assigned frequency. The IPFFT will be introduced in this section.

#### 3.4.1 Demand of Using IPFFT

Normal Fourier Transformation requires periodic and relatively steady data when moderate accuracy as one percent. Then, Discrete-Fourier Transform and Fast-Fourier Transform were utilized to obtain higher resolution and accuracy. However, these methods discussed above lead to a issue, which is called leakage effect. Therefore, IPFFT is designed for higher accuracy or poor signal quality say as noise made from hardware power source. [15]. [16]

### 3.4.2 Algorithm of Interpolated FFT

The Interpolated FFT used in this experiment focus in getting Amplitude and phase angle of the system.

Table 2 defines the parameters for arithmetic.

**Table 2** Parameter Definitions

$f_1$	fundamental frequency
$A_1$	amplitude of the fundamental frequency
$\phi_1$	phase angle of fundamental frequency
$A_n, \phi_n, n = 2, \dots$	amplitude and phase angle other than fundamental frequency
$V_{rms}$	root-mean-square value of the signal
$V_m$	average of the signal
THD	total harmonic distortion

After defining those parameters above, processes to develop the algorithm will introduce in detail later.

The equation of fundamental component define as (3.3). The DFT equation is defined as (3.4), the reverse of (3.4) is this (3.5). The DFT of (3.3) is defined as (3.6).

$$x_1(t) = A_1 \sin(2\pi f_1 t + \phi_1) \quad (3.3)$$

$$S(i) = \sum_{k=0}^{N-1} \exp(-j \frac{2\pi}{N} ik) \quad (3.4)$$

$$x(k) = \frac{1}{N} \sum_{i=0}^{N-1} \exp(j \frac{2\pi}{N} ik) \quad (3.5)$$

$$S(i) = -0.5jA_1 \{ \exp[j(a(\lambda-i) + \phi_1)] \} \frac{\sin \pi(\lambda - i)}{\sin \pi(\lambda - i)/N} - \{ \exp[-j(a(\lambda+i) + \phi_1)] \} \frac{\sin \pi(\lambda + i)}{\sin \pi(\lambda + i)/N} \quad (3.6)$$

By observing (3.6),  $a = \pi(N - 1)/N$ . (3.6) is mainly composed by two major spectral components , which are (3.7) and (3.8)

$$S(l) = -j0.5A_1 \exp[j(a\delta + \phi_1)] \frac{\sin(\pi\delta)}{\sin(\pi\delta)/N} \quad (3.7)$$

$$S(l+1) = -j0.5A_1 \exp[j(a(\delta - 1) + \phi_1)] \frac{\sin \pi(1 - \delta)}{\sin \pi(1 - \delta)/N} \quad (3.8)$$

From (3.4) through (3.8), once  $\lambda$  is not an integer, the results will not be single sinusoid results and possess  $\sin(v)/\sin(v/N)$ , which is referred to leakage effect. To solve this issue, using the same way but interpolate between  $S(l)$  and  $S(l + 1)$  of DFT components. Hence, the (3.7) and (3.8) will become (3.9) and (3.10).

$$|S(l)| = 0.5A_1 \frac{|\sin(\pi\delta)|}{\sin(\pi\delta)/N} \quad (3.9)$$

$$|S(l + 1)| = 0.5A_1 \frac{|\sin \pi\delta|}{\sin \pi(1 - \delta)/N} \quad (3.10)$$

Giving the ratio of (3.9) and (3.10) as  $\alpha$ . Substituting (3.11) by (3.9) and (3.10) gives (3.12).

$$\alpha = \frac{|S(l + 1)|}{|S(l)|} \quad (3.11)$$

$$\delta = \frac{\alpha}{1 + \alpha} \quad (3.12)$$

Thus the fundamental frequency is given as (3.13). After deducing the equation for fundamental frequency, the next step is to find the amplitude for fundamental frequency. We can be organized (3.9). (3.10) and it gives (3.14) and (3.15).

$$f_1 = \lambda f_0 = (l + \frac{\alpha}{1 + \alpha}) \frac{1}{T} \quad (3.13)$$

$$A_1 = \frac{2\pi\delta}{N} \frac{|S(l)|}{|\sin(\pi\delta)|} \quad (3.14)$$

$$A_1 = \frac{2\pi(1 - \delta)}{N} \frac{|S(l + 1)|}{|\sin(\pi(1 - \delta))|} \quad (3.15)$$

Both equation can find the amplitude for fundamental frequency, (3.15) is used when  $|S(l + 1)|$  is larger than  $|S(l)|$ .

The Interpolated FFT in this report is focus on finding the fundamental frequency, amplitude and phase angle. The phase angle can be obtained from (3.8),

$$\phi_1 = Phase(S(l)) - a\delta + \pi/2 \quad (3.16)$$

$$\phi_1 = Phase(S(l + 1)) - a(\delta - 1) + \pi/2 \quad (3.17)$$

Either of the equations can be used to find  $\phi_1$ , where  $a = \pi(N - 1)/N$ . The best way to choose the equation to apply is to use the largest spectral line.

### 3.4.3 Example of Interpolated FFT

The following results is to show an example for finding the fundamental frequency, amplitude and phase angle based on the data from RL circuit with testing  $100Hz$  voltage injection.

In the experiment, the voltage injection is  $160 Hz$  in the beginning and  $40Hz$  at  $2.5$  second in reverse phase sequence until  $5$  seconds. After finishing the simulation, the data measured from voltage on the load and current in the system will be collected and be fed into Interpolated FFT algorithm. Setting fundamental frequency as  $100 Hz$ , analyze time window as  $0.5s$ , total time as  $5s$ , so the analyze repeated for  $10$  times which take five times each for twice voltage injections. The step size is setting as  $20000Hz$ . For the first  $0.5$  second, the abc coordinates is converting to dq reference frame, the transform process contains many waveforms combination. However, IPFFT can analyze the data and give an approximate fundamental frequency, amplitude and phase angle.

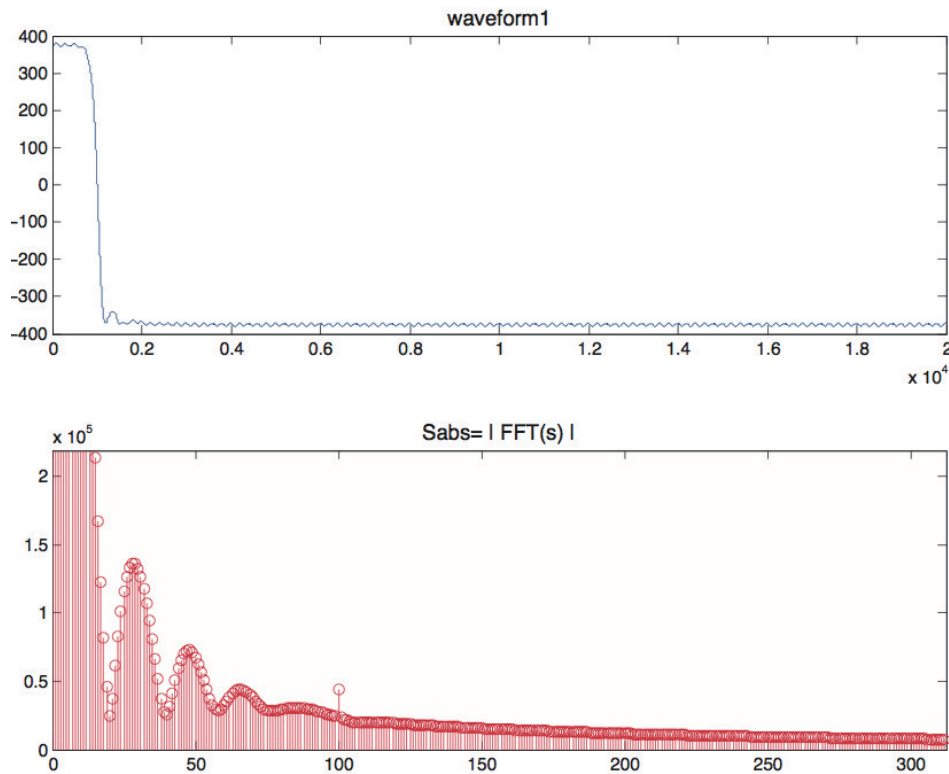


**Figure 32.** IPFFT Analysis for First 0.5 Second

After 0.5s the system is successfully transferred to D-Q coordinate, the waveform is made by DC components and 100Hz sinusoidal waveform. Since IPFFT is setting the  $f_0$  as 100Hz, so the IPFFT can focus on extracting 100Hz and filter unnecessary frequencies. Fig 33 is the diagram when system reach to steady state.

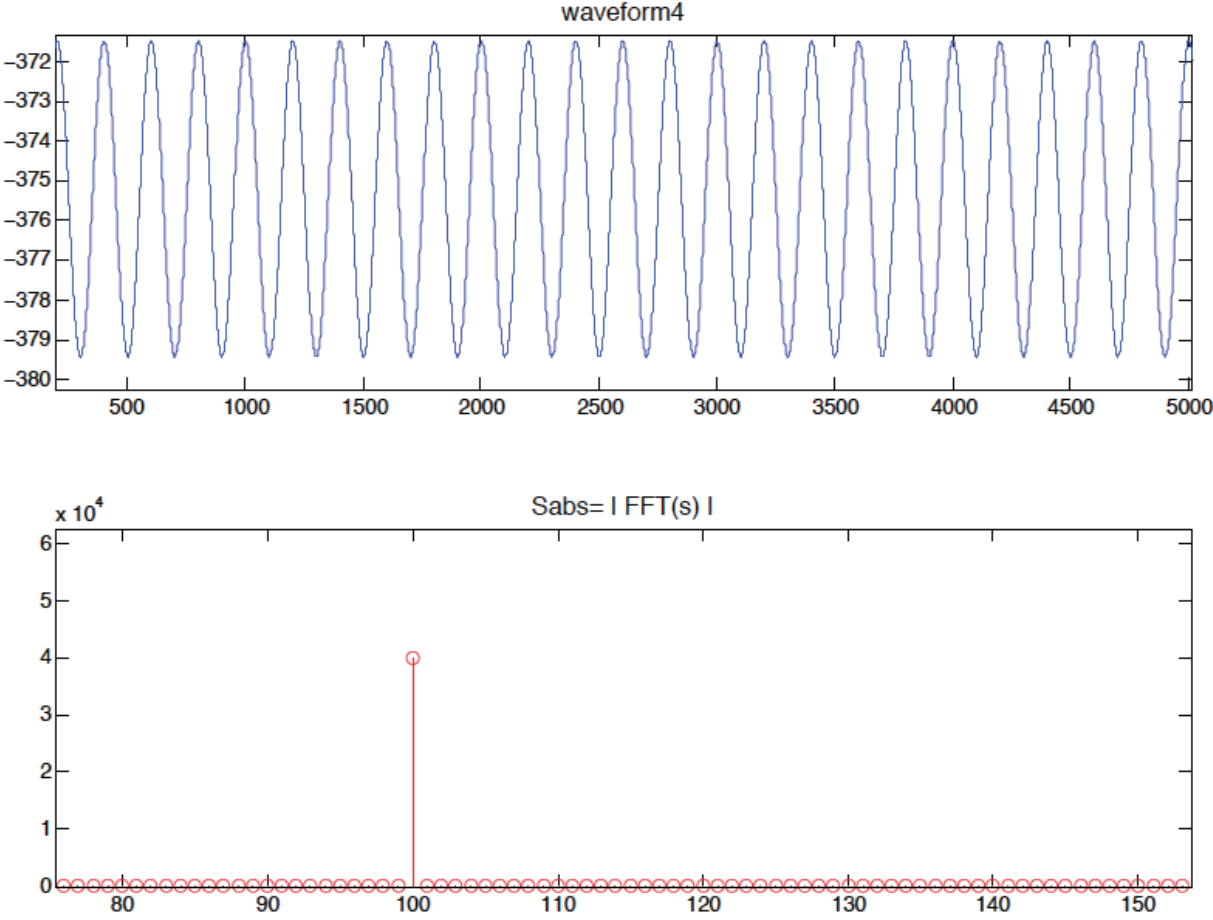


**Figure 33.** IPFFT Analysis in DQ Reference Frame

The data analysis is separated into 10 segments, each segment includes 0.5 seconds, by observing the data, the data reaches to steady and accurate after third analysis. One can take out the fourth time of analysis and use those values to obtain impedance model.

Interpolated FFT is a powerful algorithm to do the signal processing, this method can get more accurate results when the signal has other disturbance or shorter period. However, Interpolated FFT requires smaller step size compare to the normal FFT. The Interpolated FFT is introduced by this section in detail, next section will show the final experimental results.

```

***** Window Number=1 *****
1 Icase= 1 lam_ref(base 0,1,..)= 34
alpha del A1 phi1
1.04946 0.512066 13.5172 1.55961
fhat_ipfft= 66.9759

***** Window Number=2 *****
1 Icase= 1 lam_ref(base 0,1,..)= 50
alpha del A1 phi1
1.0811e-006 1.0811e-006 3.9939 1.5789
fhat_ipfft= 100

***** Window Number=3 *****
1 Icase= 1 lam_ref(base 0,1,..)= 50
alpha del A1 phi1
9.9181e-012 9.9181e-012 3.9939 1.5789
fhat_ipfft= 100

***** Window Number=4 *****
1 Icase= 1 lam_ref(base 0,1,..)= 50
alpha del A1 phi1
2.1114e-014 2.1114e-014 3.9939 1.5789
fhat_ipfft= 100

***** Window Number=5 *****
0 Icase= 0 lam_ref(base 0,1,..)= 50
alpha del A1 phi1
1.6098e-014 1.6098e-014 3.9939 1.5789
fhat_ipfft= 100

```

**Figure 34.** IPFFT Analysis in  $V_{d1}$

```

***** Window Number=6 *****
1 Icase= 1 lam_ref(base 0,1,..)= 50
alpha del A1 phi1
3.4929e-008 3.4929e-008 3.9943 1.561
fhat_ipfft= 100

***** Window Number=7 *****
0 Icase= 0 lam_ref(base 0,1,..)= 50
alpha del A1 phi1
1.1157e-013 1.1157e-013 3.9943 1.561
fhat_ipfft= 100

***** Window Number=8 *****
1 Icase= 1 lam_ref(base 0,1,..)= 50
alpha del A1 phi1
8.7252e-014 8.7252e-014 3.9943 1.561
fhat_ipfft= 100

***** Window Number=9 *****
1 Icase= 1 lam_ref(base 0,1,..)= 50
alpha del A1 phi1
1.2747e-014 1.2747e-014 3.9943 1.561
fhat_ipfft= 100

***** Window Number=10 *****
1 Icase= 1 lam_ref(base 0,1,..)= 50
alpha del A1 phi1
8.5928e-015 8.5928e-015 3.9943 1.561
fhat_ipfft= 100

```

**Figure 35.** IPFFT Analysis in  $V_{d2}$



```

1 Icase= 1 lam_ref(base 0,1,..)= 34
alpha del A1 phi1
1.0481 0.51173 1.9311 1.5599
fhat_ipfft= 66.9765

***** Window Number=2 *****

1 Icase= 1 lam_ref(base 0,1,..)= 50
alpha del A1 phi1
1.2865e-006 1.2865e-006 0.56932 1.5129
fhat_ipfft= 100

***** Window Number=3 *****

1 Icase= 1 lam_ref(base 0,1,..)= 50
alpha del A1 phi1
1.1755e-011 1.1755e-011 0.56932 1.5129
fhat_ipfft= 100

***** Window Number=4 *****

1 Icase= 1 lam_ref(base 0,1,..)= 50
alpha del A1 phi1
1.7963e-014 1.7963e-014 0.56932 1.5129
fhat_ipfft= 100

***** Window Number=5 *****

0 Icase= 0 lam_ref(base 0,1,..)= 50
alpha del A1 phi1
5.0396e-014 5.0396e-014 0.56932 1.5129
fhat_ipfft= 100

```

**Figure 36.** IPFFT Analysis in  $I_{d1}$

```

***** Window Number=6 *****

1 Icase= 1 lam_ref(base 0,1,..)= 50
alpha del A1 phi1
1.7574e-006 1.7574e-006 0.57053 1.5445
fhat_ipfft= 100

***** Window Number=7 *****

1 Icase= 1 lam_ref(base 0,1,..)= 50
alpha del A1 phi1
9.7606e-014 9.7606e-014 0.57053 1.5445
fhat_ipfft= 100

***** Window Number=8 *****

1 Icase= 1 lam_ref(base 0,1,..)= 50
alpha del A1 phi1
1.0891e-013 1.0891e-013 0.57053 1.5445
fhat_ipfft= 100

***** Window Number=9 *****

1 Icase= 1 lam_ref(base 0,1,..)= 50
alpha del A1 phi1
5.0164e-014 5.0164e-014 0.57053 1.5445
fhat_ipfft= 100

***** Window Number=10 *****

1 Icase= 1 lam_ref(base 0,1,..)= 50
alpha del A1 phi1
3.4944e-014 3.4944e-014 0.57053 1.5445
fhat_ipfft= 100

```

**Figure 37.** IPFFT Analysis in  $I_{d2}$

### 3.5 Simulation Results by MATLAB/Simulink/Simpower

This section will test the system stability in MATLAB by voltage disturbance and DQ transform. The test circuit is a basic RL circuit system, which is shown in Fig 20. The parameters are also given in Table 1. The following figures are showing impedance value in from  $1Hz$  to  $10kHz$  in d-q form and the real part and imaginary part are separately given. First, the impedance model for load impedance and source impedance are shown and split into two parts, real part and imaginary part as a benchmark as follows.

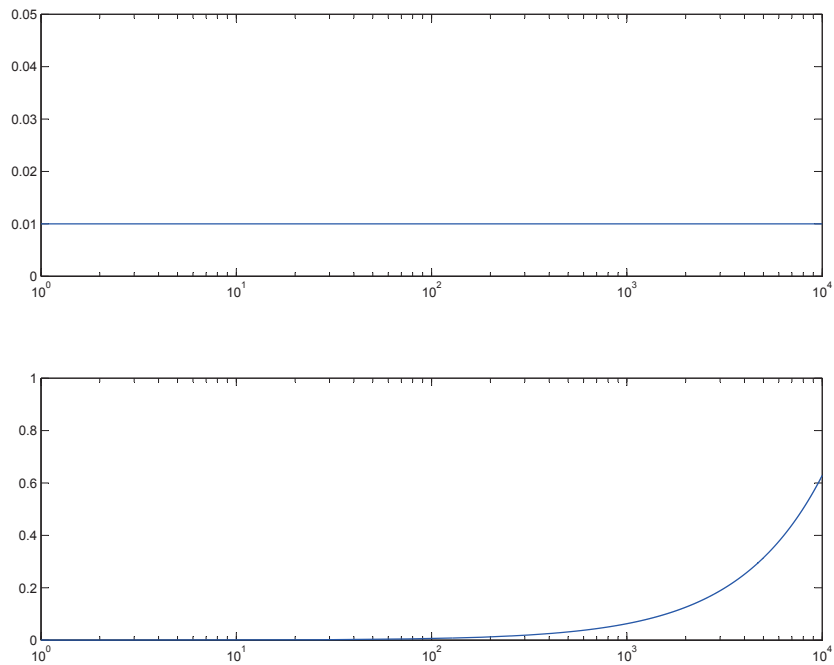


**Figure 38.** Actual Impedance Model in Real Part

The following results show the comparison between measured impedance model and actual impedance model. The red circles show the test points for RL circuit. In real part, results are pretty accurate in all frequencies. In imaginary part, results are accurate most of the time except the results from  $5000Hz$  to  $7000Hz$ . It can be fixed if we decreased the step size or voltage injection magnitude.

In these figures. Since the resistance won't be affected by frequency, Impedance in source and load show steady value as  $0.01\Omega$  and  $7\Omega$ . On the contrary, the inductance will affect the reactance if the frequency change. Hence, the imaginary value will keep increasing since this part shows the characteristics of inductor.

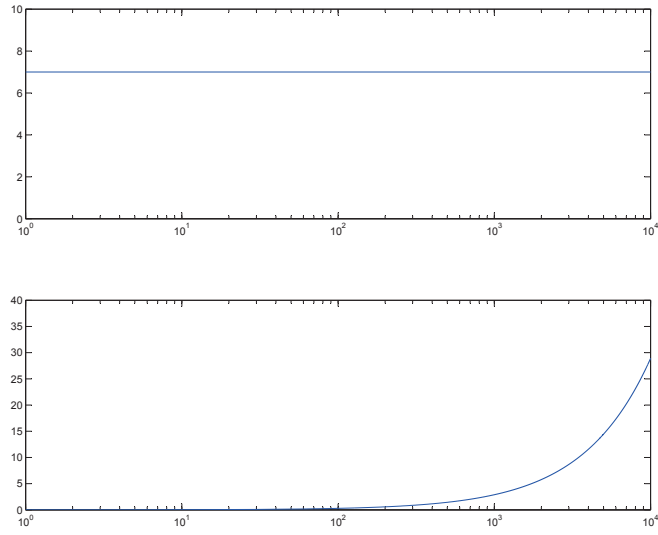


**Figure 39.** Actual Impedance Model in Imaginary Part

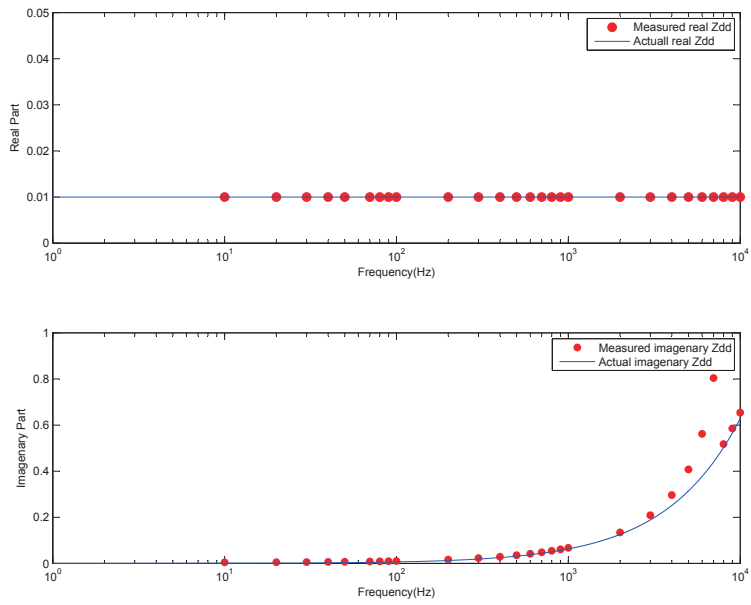


**Figure 40.** Impedance Results  $Z_{sdd}$

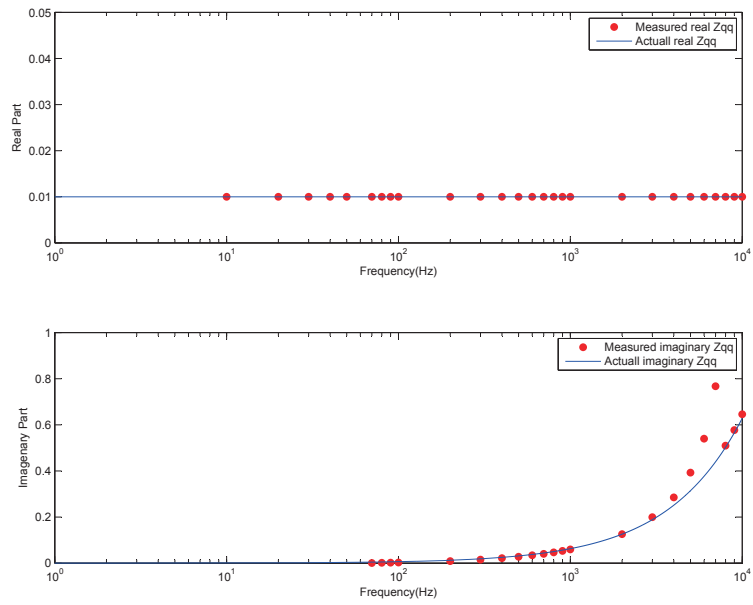


**Figure 41.** Impedance Results  $Z_{sqq}$

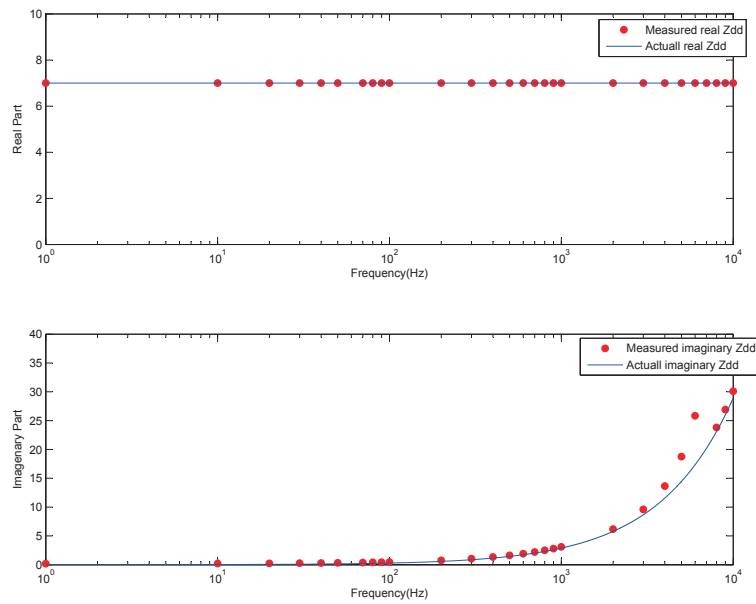


**Figure 42.** Impedance Results  $Z_{idd}$

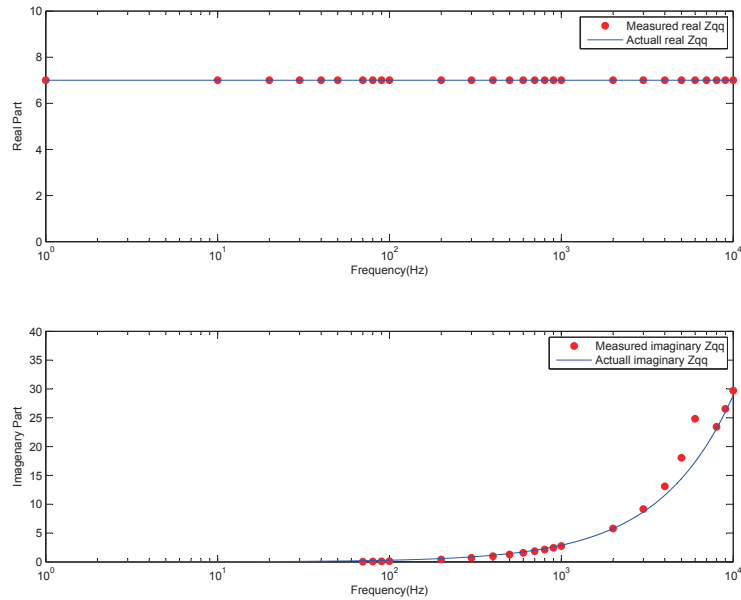


Figure 43. Impedance Results  $Z_{lqq}$

### 3.6 Case Study: AC/DC/AC Converter

Based on successfully measure the impedance through Impedance extraction method. Further application will be tested, especially testing the system with power electronics which have negative impedance characteristics. An AC/DC/AC converter is built by Simpower and the diagram and parameters is given as Fig 44 and Table 3.

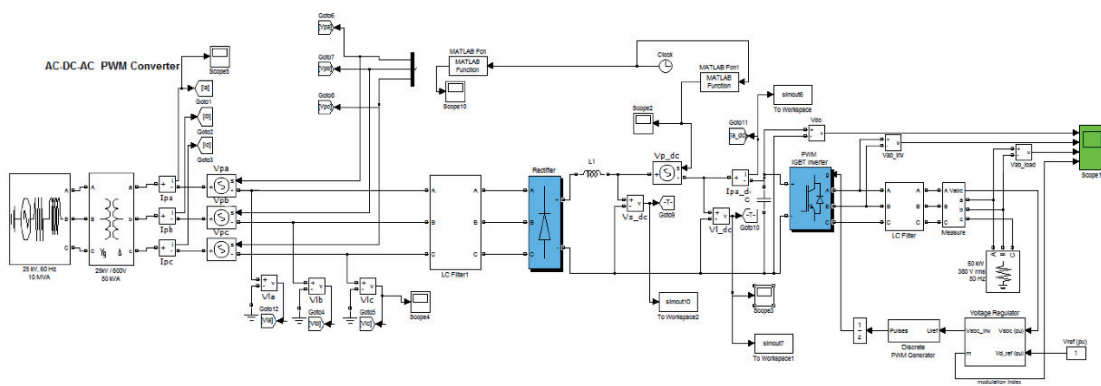


Figure 44. AC to DC to AC Converter Circuit Diagram

**Table 3** Parameter for AC/DC/AC Converter

Three Phase Source	25kV, 60Hz, 10MVA
Three Phase Transformer	500V, 50kVA
Source resistor	13.15Ω
Source inductance	20mH
Source capacitance	200μF
Load resistor	13.15Ω
Load inductance	2mH
Load capacitance	20μH
Inductance in DC side	0.2mH
Capacitance in DC side	5000μF
Rectifier modulation index	0.8
Inverter modulation index	1
Peak injected voltage	10V
Testing Frequency Range	1Hz – 10kHz

Testing frequency for 200Hz as an example, disturbance voltage frequency for the first time is 260Hz, second time is 140Hz. Voltage measured after injection in phase C is shown as Fig 46.

Since the rectifier modulation index is 0.8 so the voltage transfer to DC voltage is 400V. Fig 47 shows the results of the operation of the converter and voltage waveform after filter.

Finally, the impedance model for AC/DC/AC converter are shown for the following diagram in source side and load side separately. The real part and imaginary part are taken apart. For source impedance, the result is similar to results as previous example RL circuit since the source impedance is RLC circuit. The load side contains a rectifier and a converter so the impedance model has been extracted by the voltage disturbance. Which are shown in following diagrams.

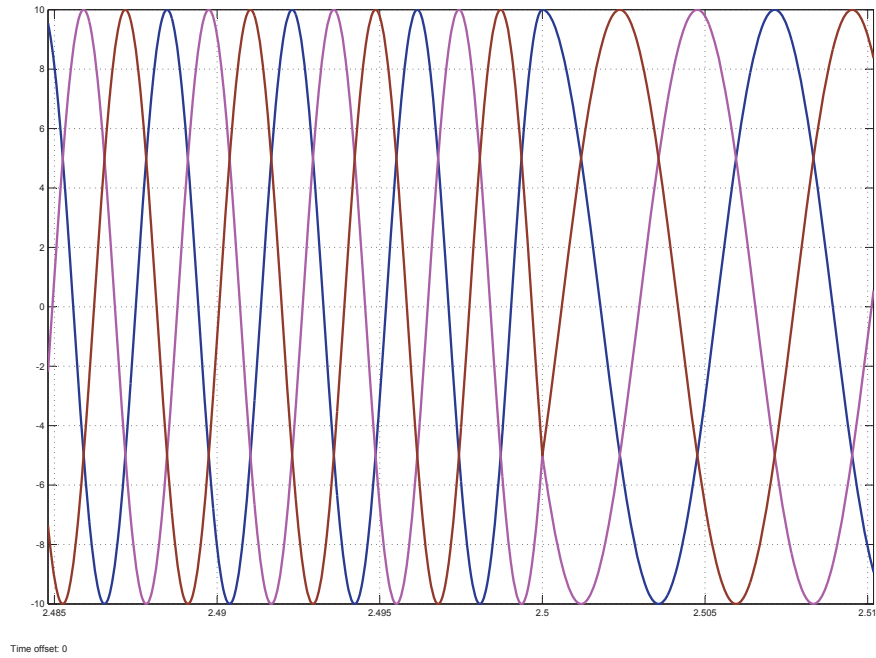


**Figure 45.** Voltage Injection for AC/DC/AC Converter

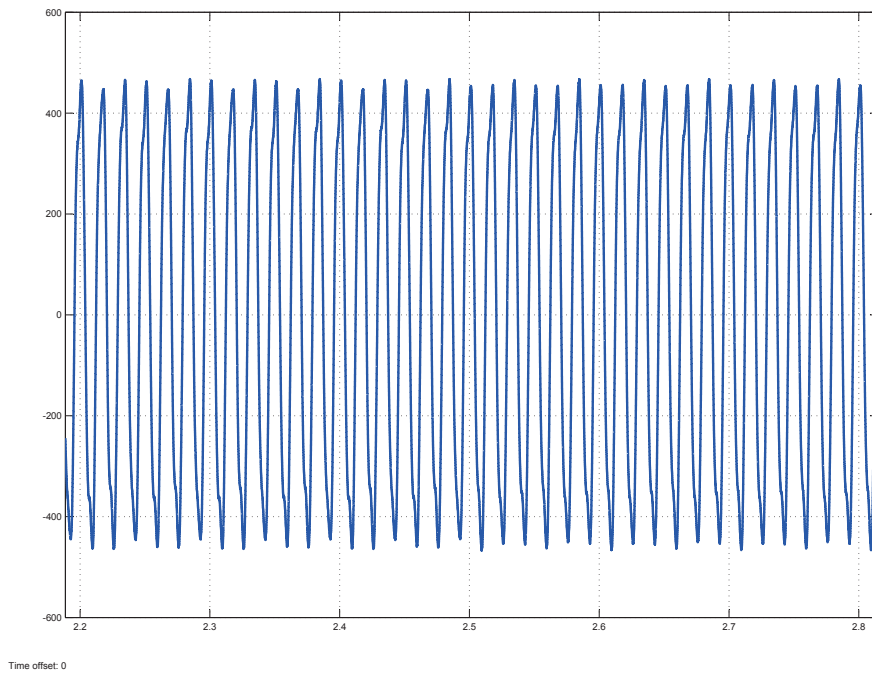
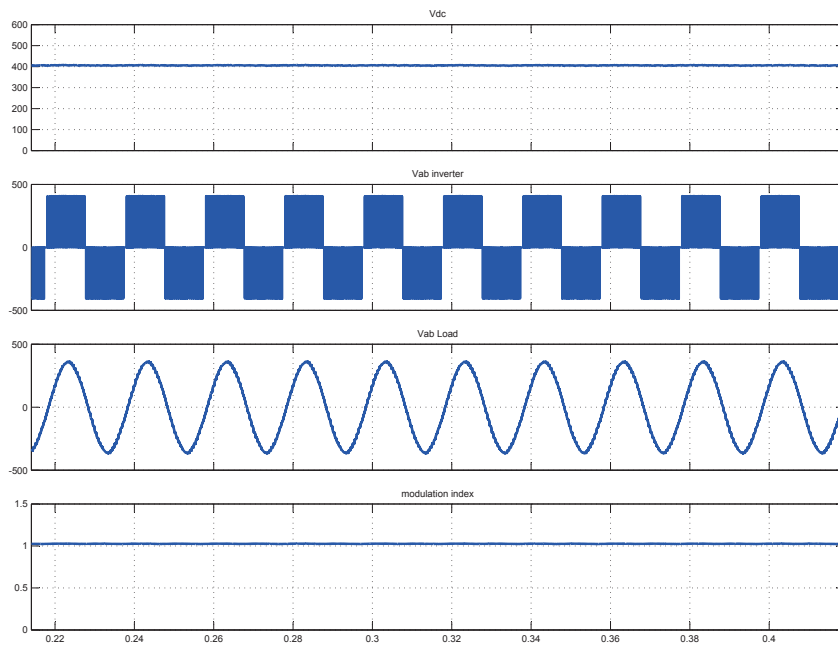


**Figure 46.** Voltage Measurement after Disturbance



Time offset: 0

**Figure 47.** Output of AC/DC/AC Converter

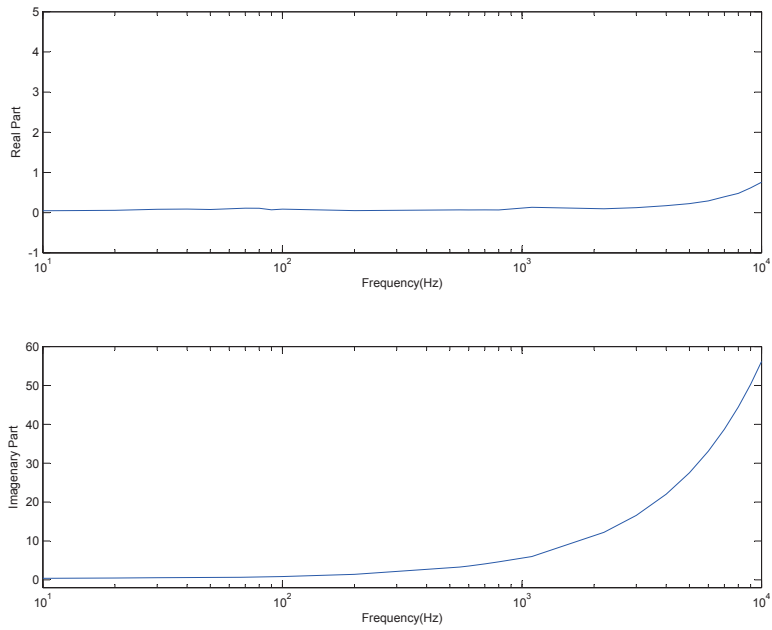


**Figure 48.**  $Z_{sdd}$  for AC/DC/AC Converter



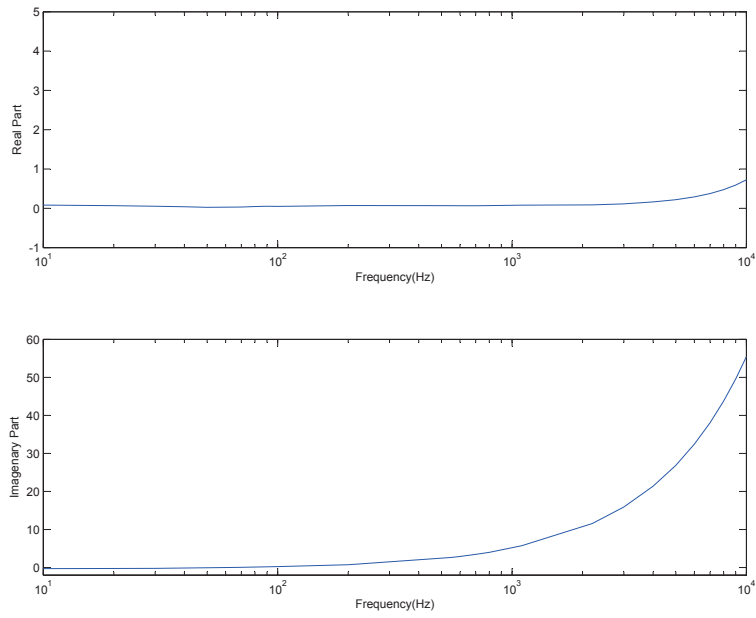


**Figure 49.**  $Z_{sqq}$  for AC/DC/AC Converter

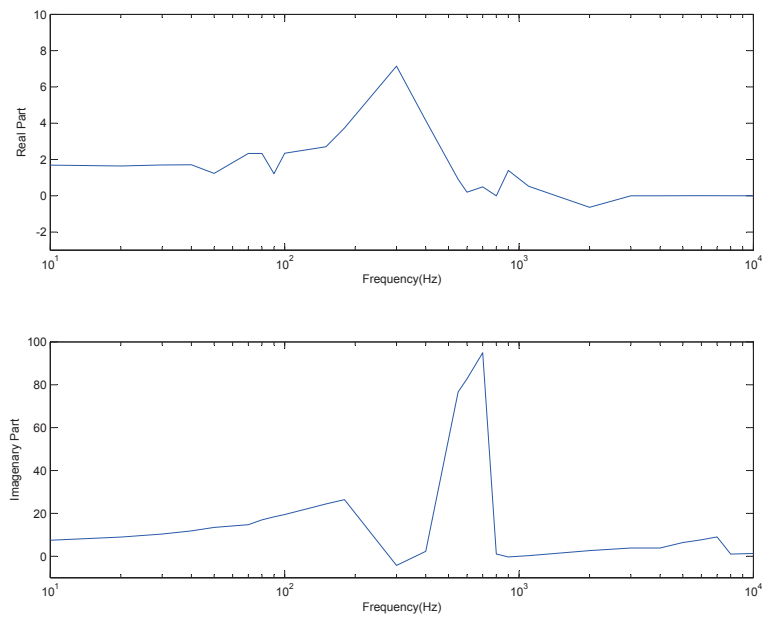


**Figure 50.**  $Z_{ldd}$  for AC/DC/AC Converter

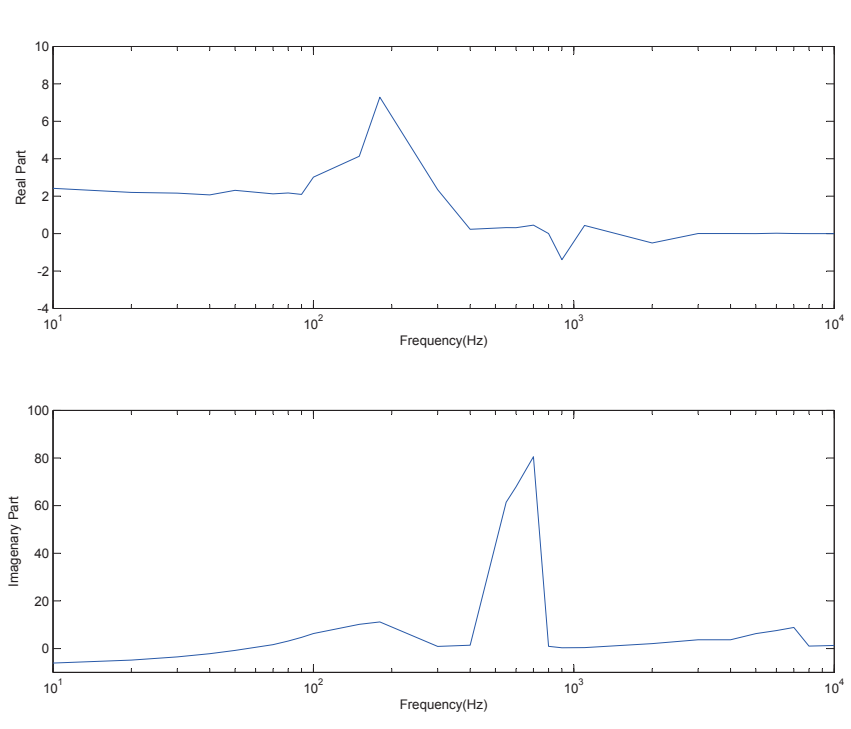


**Figure 51.**  $Z_{lqq}$  for AC/DC/AC Converter

## Chapter 4

### Impedance Extraction Algorithm Architect by LabView and Multisim

This chapter will introduce the algorithm programming on LabView and used Multisim to build a circuit model. The purpose to use LabView is testing the hardware system AC/DC/AC converter for single board made by National Instrument. The purpose to use Multisim is drawing the circuit model to run the simulation before testing on the hardware. The first section will introduce Multisim model design and configuration. Second section will introduce LabView D-Q transform algorithm design, and last section will show experiment results to verify previous result by MATLAB/Simulink.

#### 4.1 Multisim Circuit Model and Configuration

Multisim is a computer aided design software. The software has the same properties as Simpower, but it is closer to real life components since it can choose the real world model type and brand for power electronics, impedance models and power supplies. Take simple RL circuit as an example to start. The RL circuit is shown as Fig 51 and the parameters are shown as Table 4.

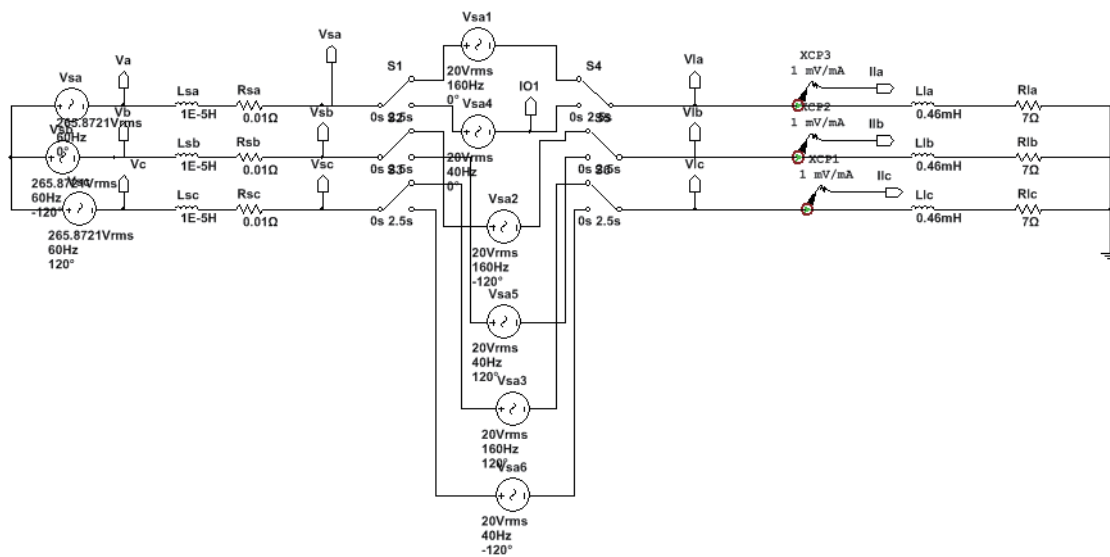


Figure 52. RL Circuit Built by Multisim

**Table 4** RL Circuit Parameters

RMS source voltages	265.8V
RMS injection voltages(per phase)	20 V
Source resistance	0.01 $\Omega$
Source inductance	10 $\mu H$
Load resistance	7 $\Omega$
Load inductance	460 $\mu H$
Testing Frequency Range	1Hz – 10kHz

The circuit model is composed by a three-phase balanced source connected to a three phase source impedance and load impedance. The disturbance is injected between the source impedance and the load impedance and voltage measurements is installed before and after the disturbance. Current measurements can be put in either way of the circuit since the current on each side will obtain the same results. After constructing a RL circuit model in Multisim, the algorithm architect can build in LabView to do the co-simulation.

## 4.2 LabVIEW Algorithm Architect

LabVIEW is a powerful system-design platform and development environment for a block diagram programming language. By using dataflow programming and graphical programming, LabVIEW can be used for automation control, data acquisition, and industrial automation. LabVIEW is also a very flexible software which can parallel program with other computer language software like MATLAB and Multisim. In this chapter, all of software mentioned before will be used and collaborated with each other. First, circuit model will be built by Multisim as test beds. Then, power electronics control, phase-locked loop, Park transform, and data collection are designed by LabVIEW. Finally, the data are analyzed by using Interpolated Fast Fourier Transform on MATLAB platform.

### 4.2.1 Parallel Programming Output

The circuit model has been built by Multisim, one significant feature of Multisim and LabVIEW is co-simulation. The LabVIEW can read the Multisim file to run the circuit model and connect inputs and outputs in LabVIEW's vi.

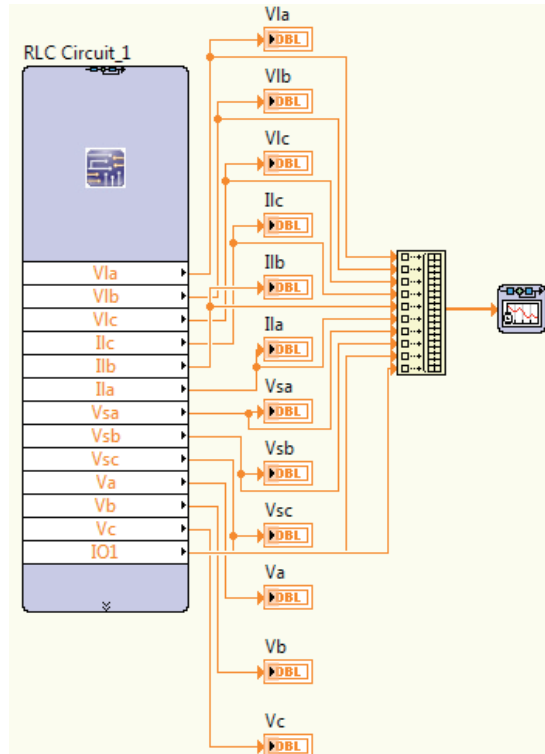


**Figure 53.** LabVIEW I/O Interface with Multisim

#### 4.2.2 Phase-Locked Loop and Ramp Signal

LabVIEW vi has build-in PLL algorithm, by giving each source phase signal, step size and, PI gain parameters, PLL can lock the source frequency.

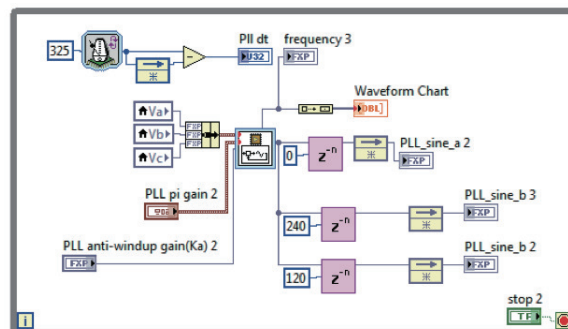


**Figure 54.** Phase-Locked Loop in LabVIEW

The frequency from PLL can be used to create a ramp signal by simulate sin-waveform and cosine-waveform and divide first one from second one. With time various, the results will be a rotating cycle from  $-180$  degree to  $180$  degree.

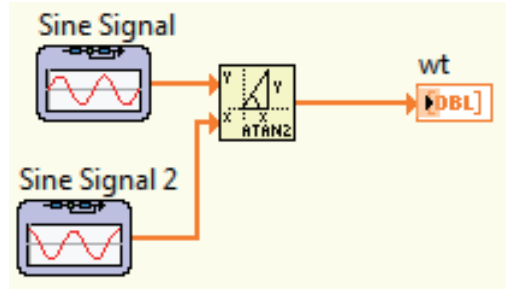


**Figure 55.** Ramp Signal Created by LabVIEW

Ramp signal is obtained from sinusoidal waveform, the values are represented by degree. Then, change the unit from degrees to numbers,  $-180$  degree can be rewritten as  $-\pi$  and  $180$  degree can be rewritten as  $\pi$ .

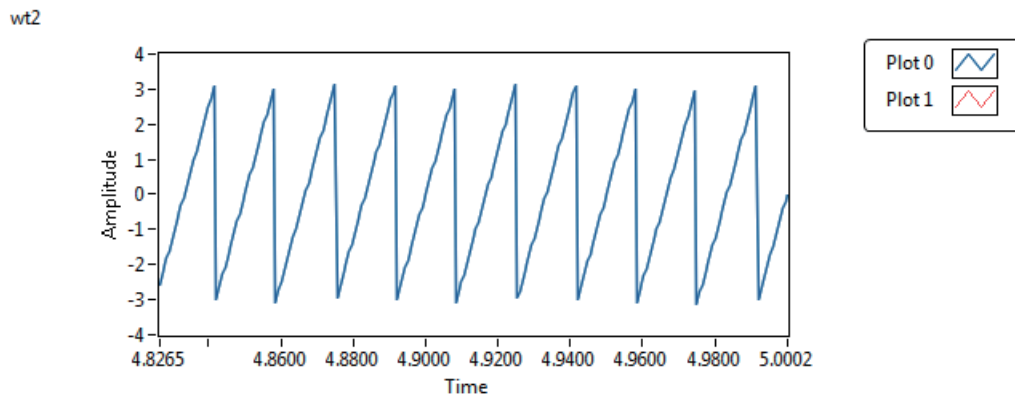


**Figure 56.** Ramp Signal Result in LabVIEW

### 4.2.3 Park Transform

LabVIEW can use MATLAB code, which is called MathScript vi, using Park transform equation in (2.22) and the algorithm is showed Fig 57.

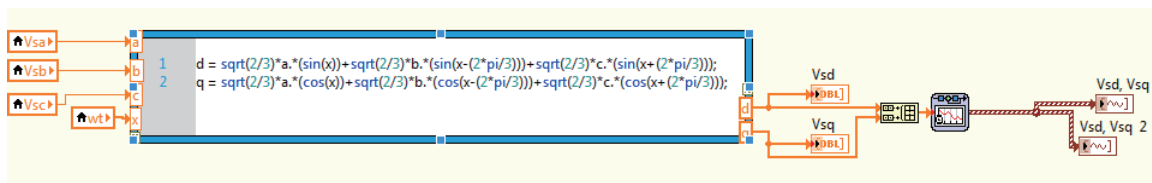


**Figure 57.** Park Transformation in MathScript

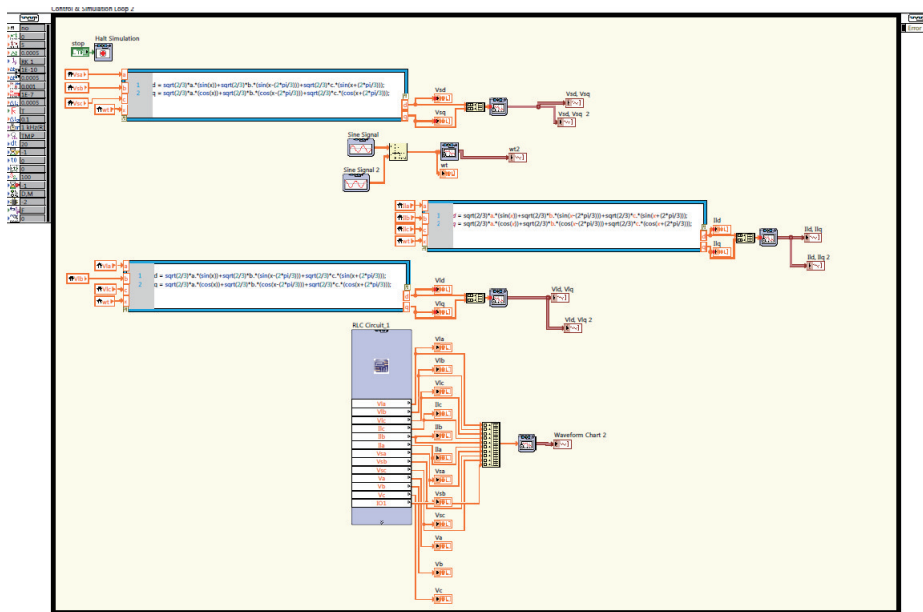


Figure 58. Ramp Signal Algorithm in LabVIEW

Vsd, Vsqr 2

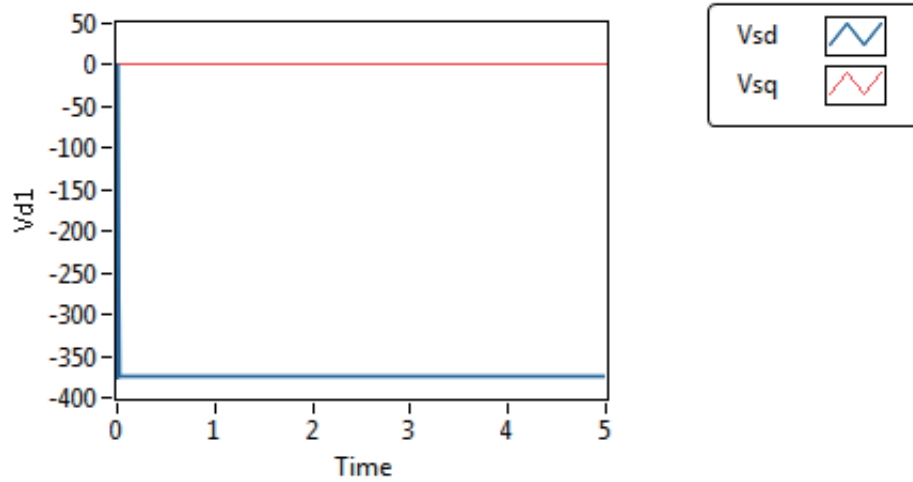
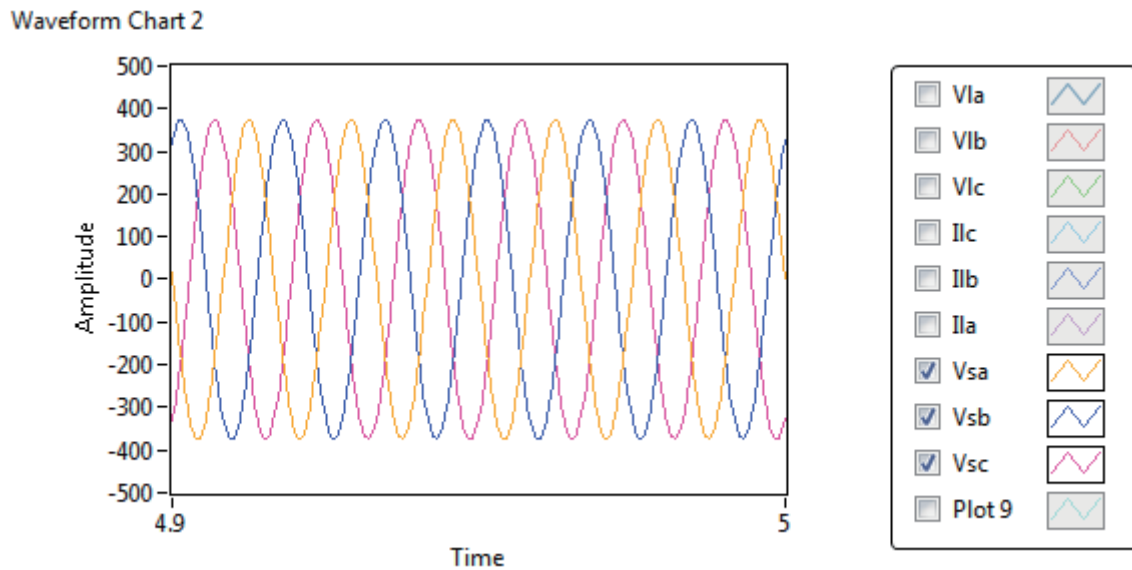


Figure 59.  $V_d$  and  $V_q$  After Park Transform

### 4.3 Results and Analysis

Fig 60 shows the three-phase balanced system without any disturbance. The circuit test bed was built by Multisim and controlled by LabVIEW, the figure only shows three phases of voltages in order to clearly define the situation. The three-phase balanced voltage source are 376 in magnitude and each phase delays with 120 degree.



**Figure 60.** Three-Phase Balanced Voltage Source

Injected Voltage to make a disturbance, and chose peak voltage as 4 in order not to make system unstable, the test frequency is from  $10\text{Hz}$  to  $7\text{kHz}$ . After signal processing by Park transform. The results are shown as Fig 62 to Fig 65. The artificial reference frame has been created in D-axis and Q-axis, voltages and currents represent as  $V_d$ ,  $V_q$ ,  $I_d$ , and  $I_q$ .

Collecting data from LabVIEW and do the IPFFT and solve matrices to obtain impedance model. In these figures, since the resistance won't be affected by frequency, Impedance in source and load show steady value as  $0.01\Omega$  and  $7\Omega$ . On the contrary, the inductance will affect the reactance if the frequency change. Hence, the imaginary value will keep increasing since this part shows the characteristics of inductor.

Fig 66 to Fig 71 shows a series of simulation results operating by LabView and Multisim. First two figures show the actual impedance model by computer calculation given parameters. Last four figures are comparison between actual results and simulated results where solid blue lines represent actual result and red dots represent tested results



Waveform Chart 2

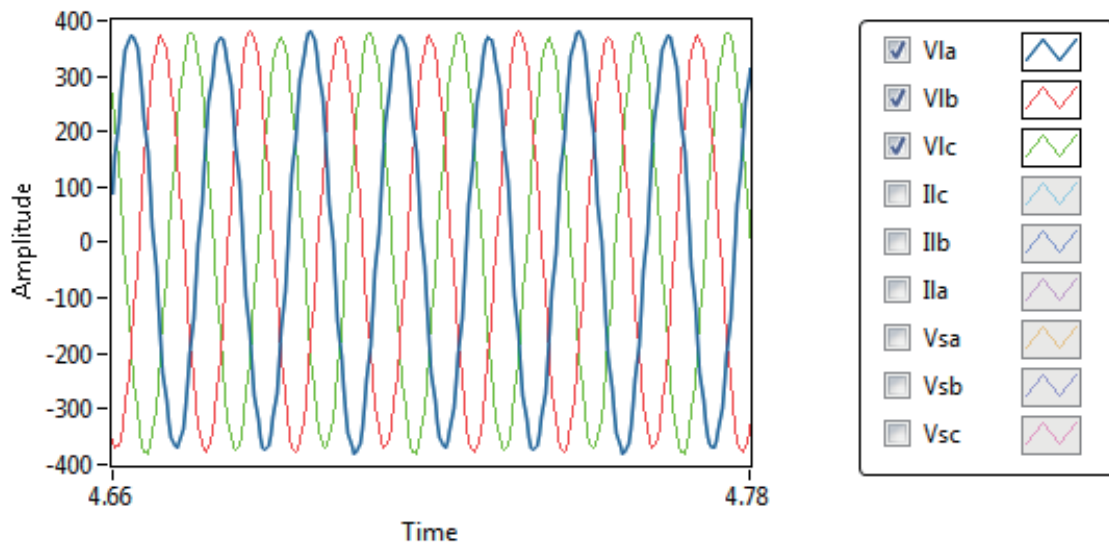


Figure 61. Load Voltages with Disturbance

V<sub>d</sub>, V<sub>q</sub> 2

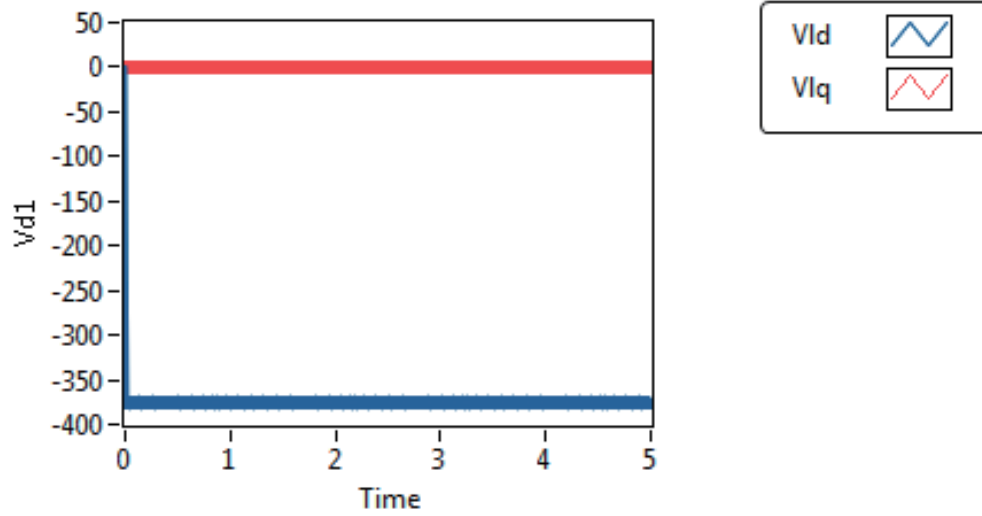
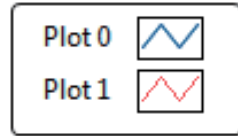
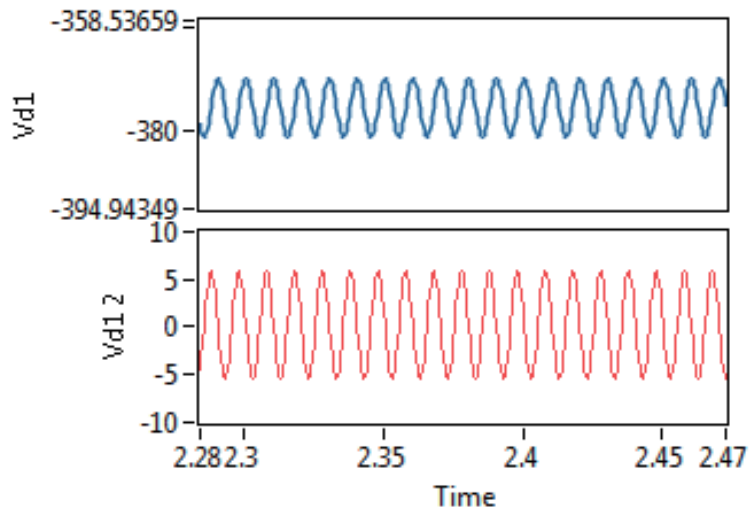


Figure 62.  $V_d$  and  $V_q$

V<sub>d</sub>, V<sub>q</sub>



**Figure 63.**  $V_d$  and  $V_q$  in Detail

I<sub>d</sub>, I<sub>q</sub>

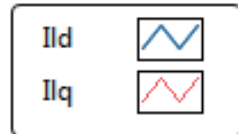
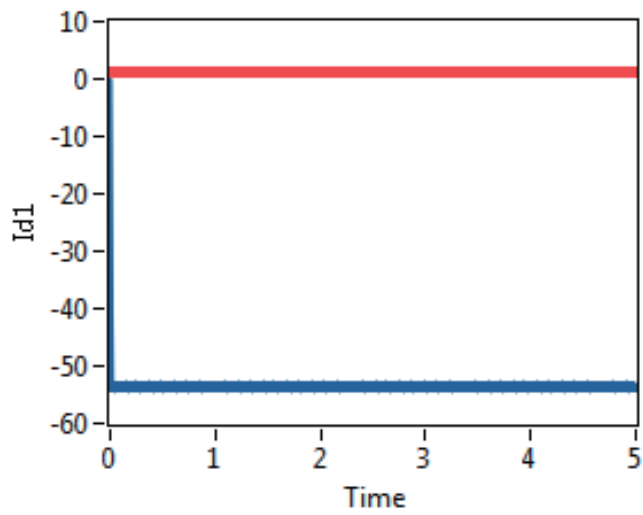


**Figure 64.**  $I_d$  and  $I_q$

I<sub>d</sub>, I<sub>q</sub>

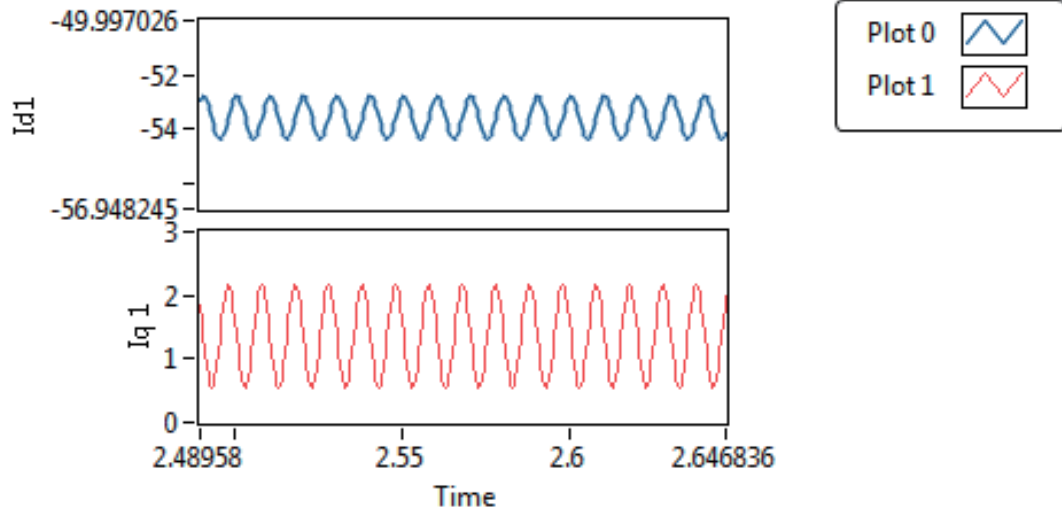


**Figure 65.**  $I_d$  and  $I_q$  in Detail

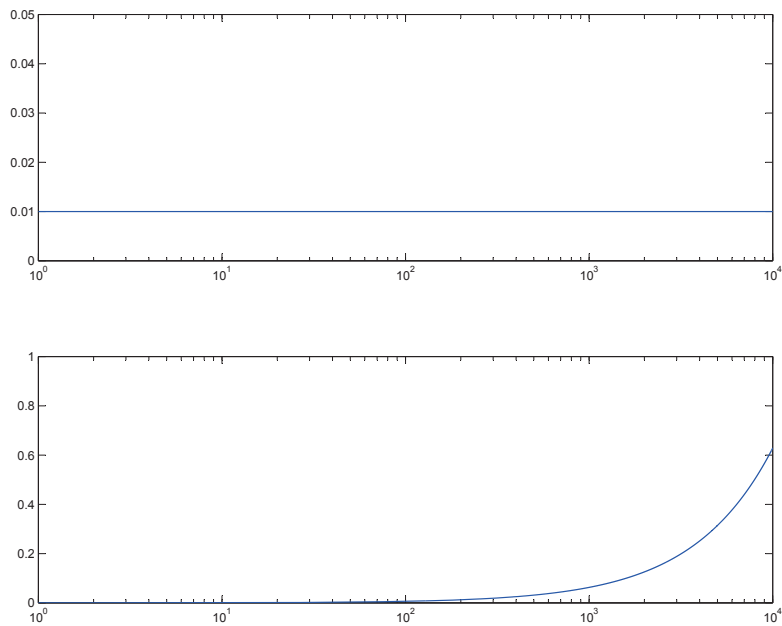


**Figure 66.** Actual Impedance Model in Real Part

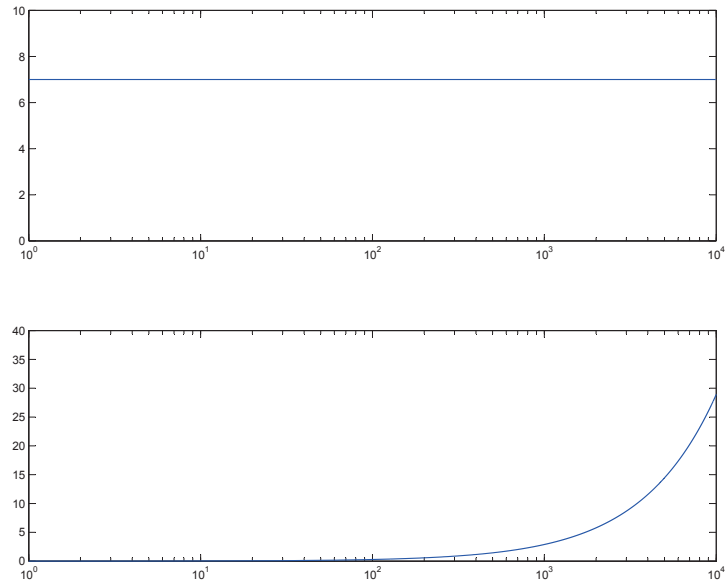


**Figure 67.** Actual Impedance Model in Imaginary Part

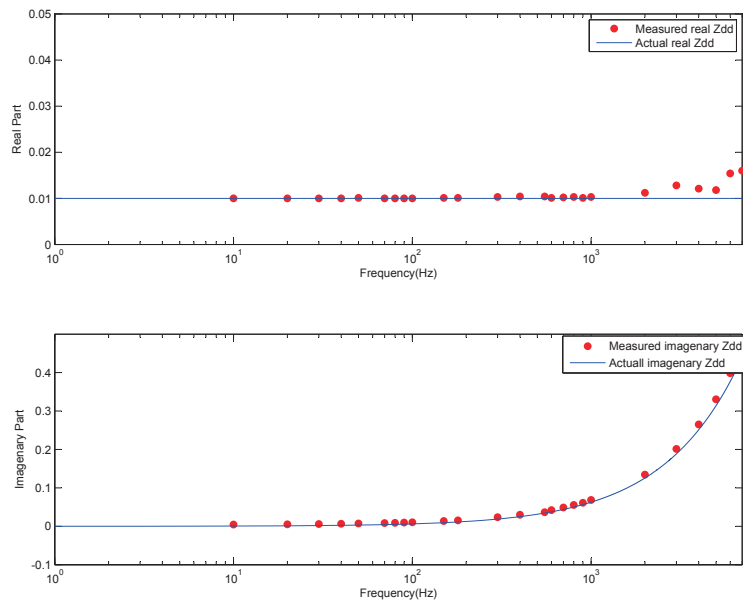


**Figure 68.**  $V_{sdd}$  Impedance Model

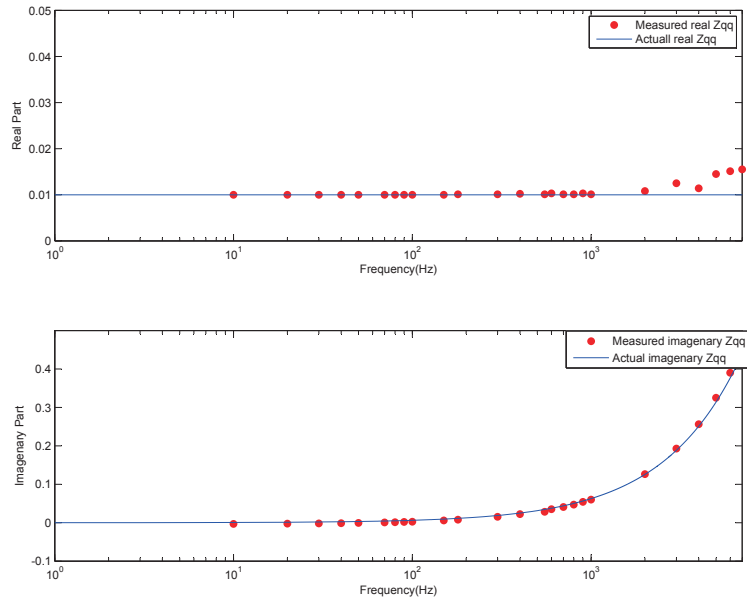


**Figure 69.**  $V_{sqq}$  Impedance Model

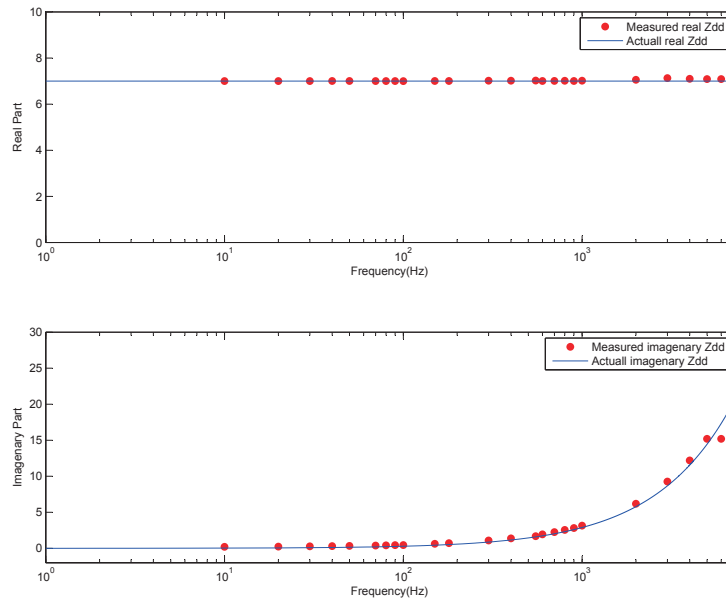


**Figure 70.**  $V_{idd}$  Impedance Model

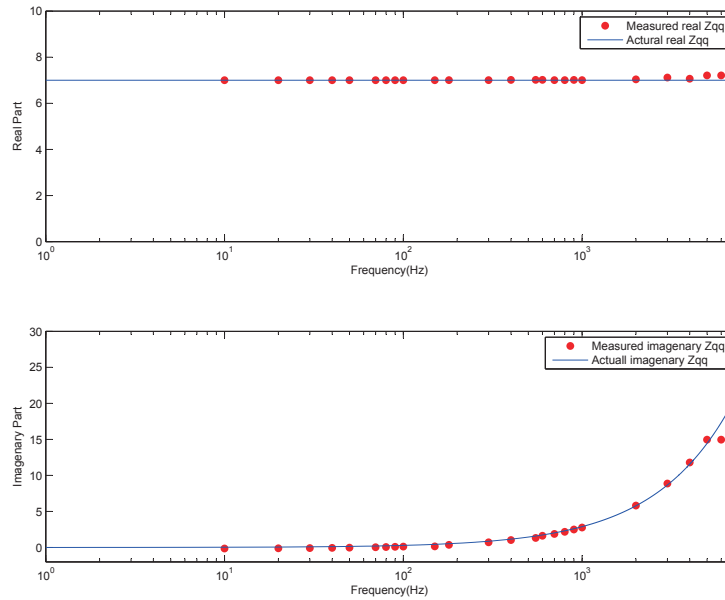


**Figure 71.**  $V_{lqq}$  Impedance Model

#### 4.4 Case Study

After successfully building the algorithm to test the impedance model on LabVIEW, the DC/AC inverter and AC/DC rectifier are case studies for further application. The algorithm can be summarized by the following diagram as fig 72. The first case study is AC/DC rectifier, circuit diagram and configure parameters

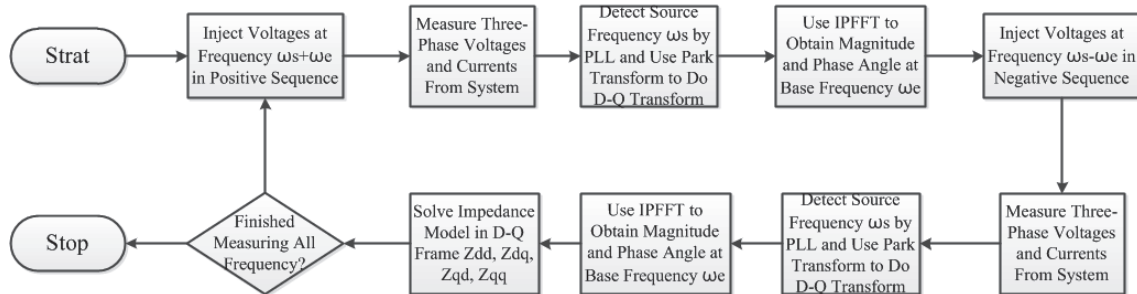


**Figure 72.** Impedance Extraction Algorithm

are given in Table 5.

Impedance on load side represents the synchronous generator, impedance before rectifier is a filter. Since the source frequency is  $60Hz$ , the current measurement is composed by harmonics based on  $60Hz$ . Impedance

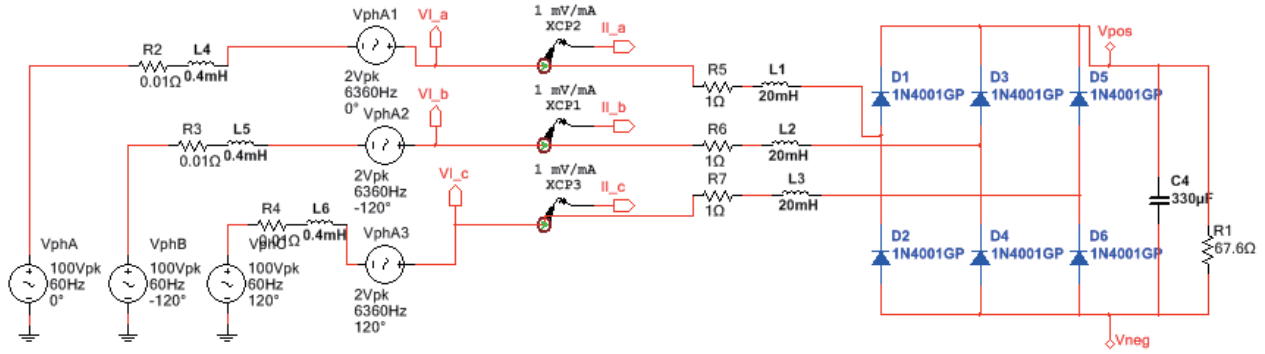


**Figure 73.** AC to DC Rectifier Circuit Diagram

**Table 5** AC to DC Rectifier Parameters

Peak source voltages(per phase)	100V
Peak injection voltages(per phase)	2V
AC source frequency	60Hz
Source resistance	0.01Ω
Source inductance	0.4mH
Load resistance	1Ω
Load inductance	20mH
Load resistance in DC	67.6Ω
Load inductance in DC	330μF
Testing Frequency Range	10Hz – 7kHz

extractions in frequencies close to multiples of 60Hz will be affected and will cause accuracy issue, which has the results similar to DC component. The impedance model results are shown from Fig 74 through Fig 77.

The second case is DC/AC inverter, which is transform DC power into AC power. The circuit topology describes as follows, DC voltage power sources connected to three-phase full bridge DC/AC inverter, RLC filter was connected to the system in order to get better waveform. Load, represents the synchronous generator, was connected after the filter, injected voltages installed between load and filter. Last, current measurements installed on both sides of injection. To fulfill this experiment, the circuit test bed was built by Multisim and co-simulation with LabView. The LabView focus on control signal and data extraction. Results were taken out and analyzed by matlab using Interpolated FFT. Circuit diagram and configure parameters are given as Table 6 and Fig 78. The impedance model in D-Q reference frame results are shown from Fig 79 to Fig 82.

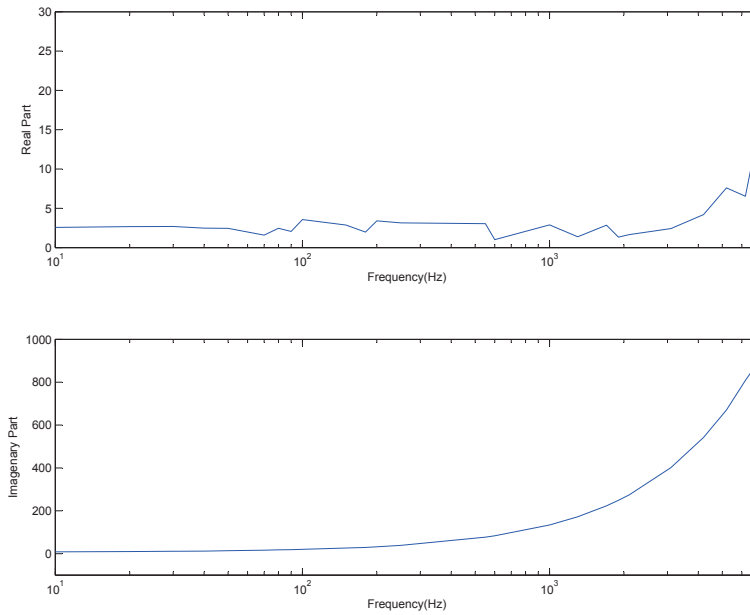


**Figure 74.**  $V_{sdd}$  Impedance Model for AC/DC Rectifier

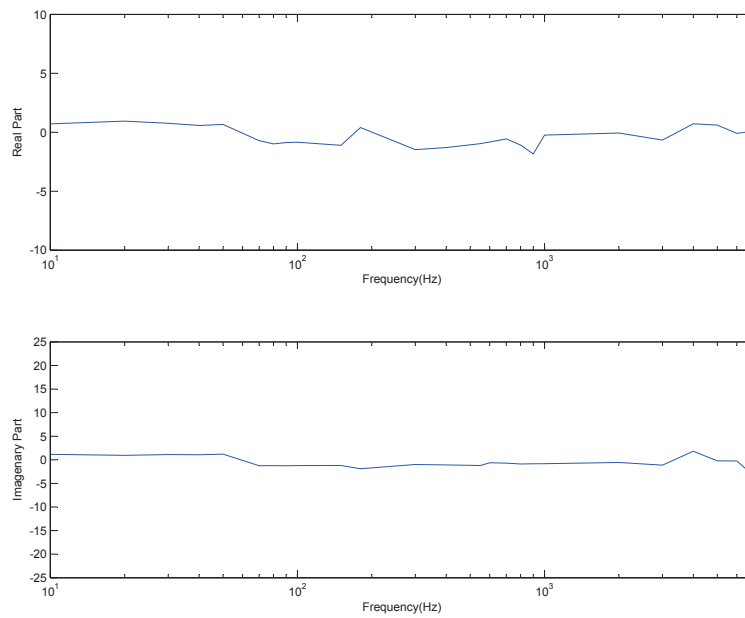


**Figure 75.**  $V_{sdq}$  Impedance Model for AC/DC Rectifier



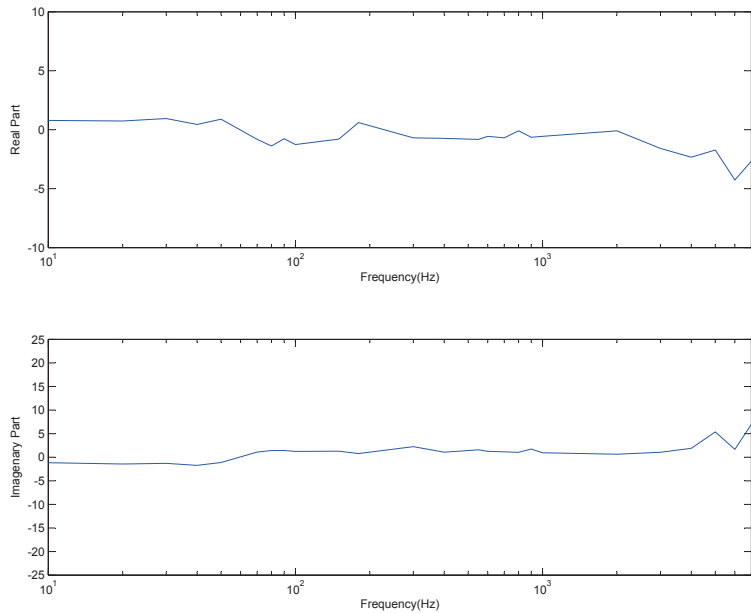


**Figure 76.**  $V_{sqd}$  Impedance Model for AC/DC Rectifier

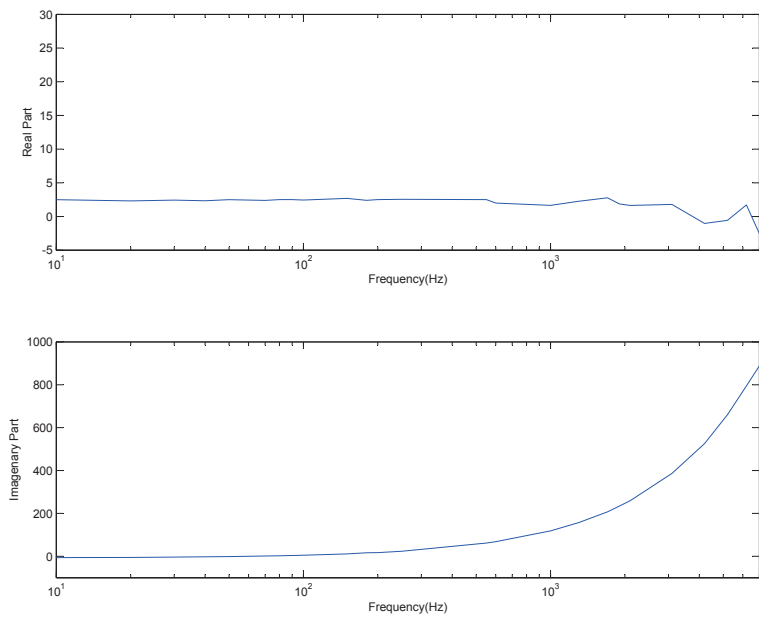


**Figure 77.**  $V_{sqq}$  Impedance Model for AC/DC Rectifier

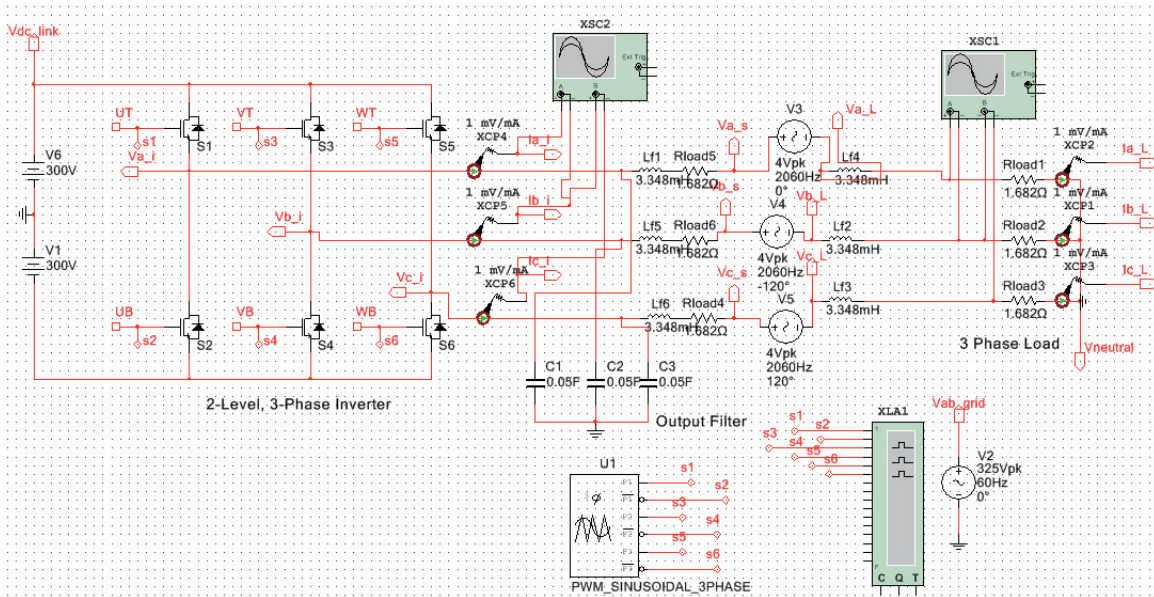


**Figure 78.** DC to AC Inverter Circuit Diagram

**Table 6** DC to AC Inverter Parameters

Source DC voltages	600V
Peak injection voltages(per phase)	4V
Source resistance	1.682Ω
Source inductance	3.348mH
Source capacitance	5μF
Load resistance	1.682Ω
Load inductance	3.348mH
Modulation frequency	60Hz
Testing Frequency Range	10Hz – 7kHz

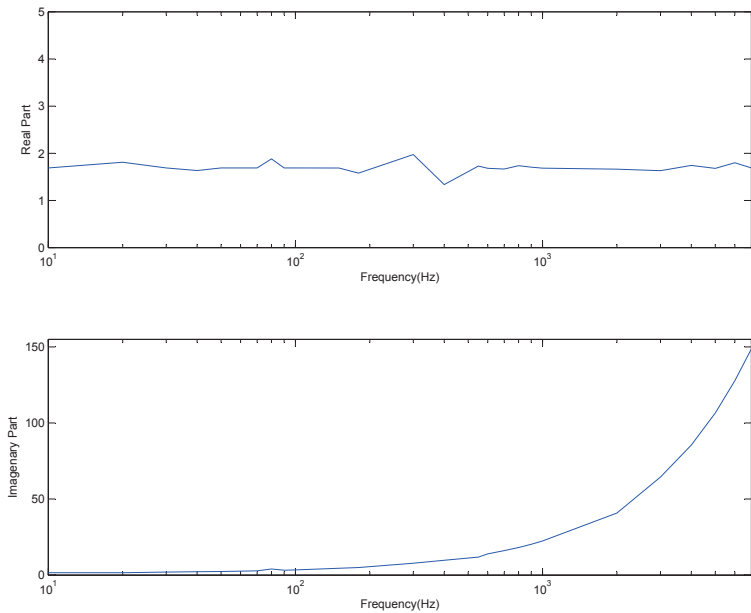


**Figure 79.**  $V_{sdd}$  Impedance Model for DC/AC Inverter

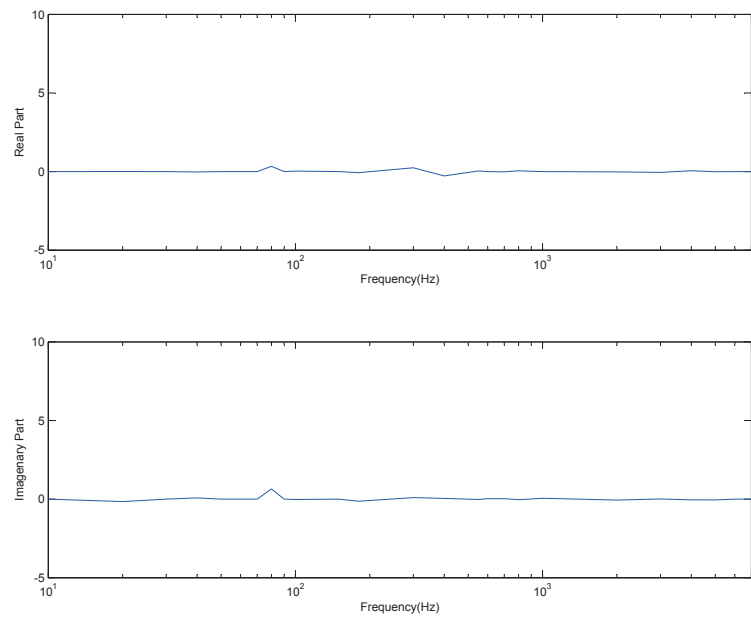


**Figure 80.**  $V_{sdq}$  Impedance Model for DC/AC Inverter

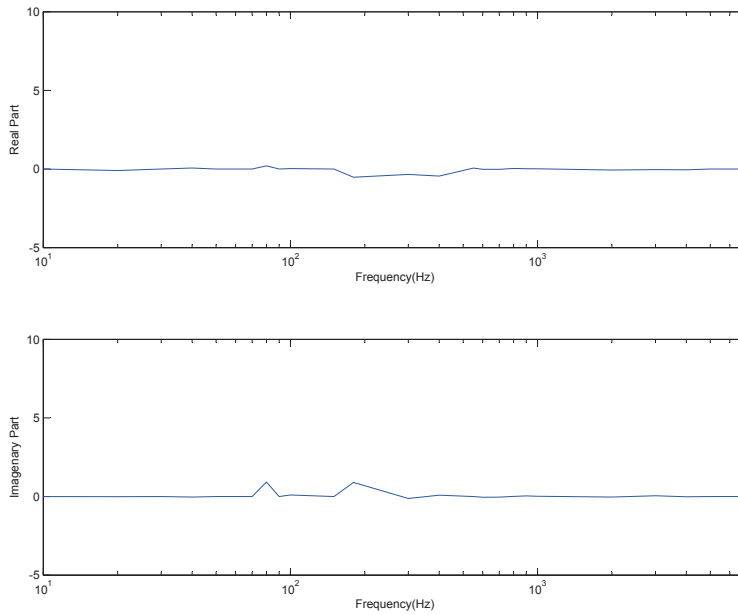


**Figure 81.**  $V_{sqd}$  Impedance Model for DC/AC Inverter

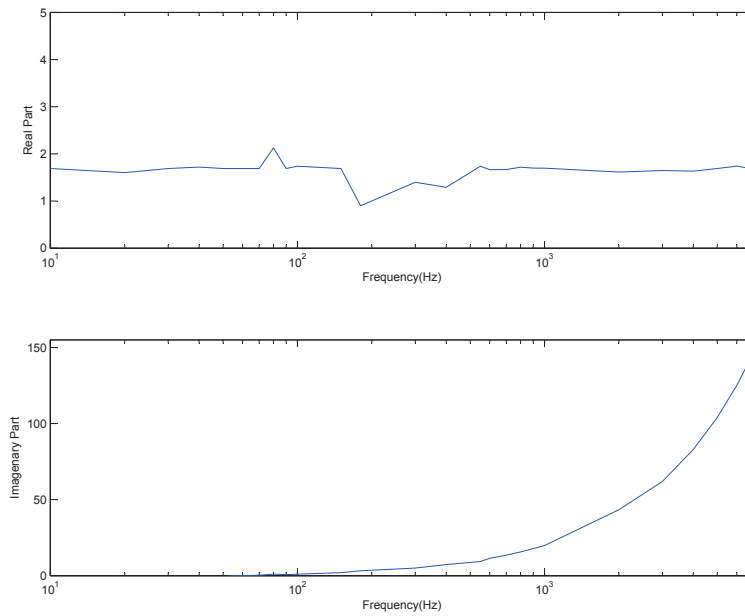


**Figure 82.**  $V_{sqq}$  Impedance Model for DC/AC Inverter

## 4.5 Summary and Conclusions

In this chapter, algorithm has been built in both MATLAB and LabVIEW, Multisim plays a important role as a test bed and cooperates with LabVIEW. In LabVIEW, PLL is designed to lock source frequency and produce ramp signal. Impedance has been changed based on PLL alignment. The Park Transform coded by MATLAB code created an imaginary reference frame to D- axis and Q- axis and impedance model is aligned on D-Q frame.

## **Chapter 5**

### **Summary and Conclusions**

#### **5.1 Summary**

This report has reviewed a basic three-phase balanced system and dynamics of active loads. A DQ reference frame has been briefly addressed in this chapter as well. The objective to do impedance extraction has been given in detail in Chapter 1.

The injection method and principle has clearly explained in Chapter 2, including both the voltage model and the current injection model. Injecting selection has been explained by equation and vector diagram, algorithm step and impedance matrix calculation are also written down in detail.

The algorithm architect has been built by MATLAB in Chapter 3. The algorithm includes Phase-Locked Loop, Park Transform, and Interpolated Fast Fourier Transformation. Fast Fourier Transformation applied in the report is to pursue even more accurate analysis. Finally, a simple RL circuit model is under the test to verify the experimental approaches. An AC/DC/AC converter model has been tested as a real-life application.

Chapter 4 demonstrated the way to implement impedance extraction in the LabVIEW platform. Multisim, cooperating with MATLAB, has drawn the circuit model and controlled by LabVIEW, using FPGA design to control the circuit in Multisim and collect data to do IPFFT on MATLAB and further impedance calculation. The algorithm with PLL, Ramp Signal, Park Transform, also designed in LabVIEW platform. A RL circuit the same as MATLAB has been tested and results are verified by the circuit parameters. Further case study as AC/DC rectifier and DC/AC inverter has been tested in this chapter.

#### **5.2 Conclusions**

The impedance in D-Q reference frame can be obtained by injecting different frequency of voltage to make a perturbation. Measuring voltages and currents on load or source interface through system's response to the particular perturbation injected and transferring voltages and currents from ABC to D-Q reference

frame. Acquiring all data and store data to do post-processing. After collecting all necessary data. The impedance calculation and bode plot can be made via data storage and obtain the impedance model in D-Q reference frame.

When acquiring these measurements, the frequency of injection can cause voltages and currents difference in the D-Q reference frame. The frequency difference is the difference between the injected frequency and line frequency. As a consequence, the system will be unstable if the injected frequency is close to the line frequency or multiple of line frequency. The transform will become to saturate and cause error.

During the process of measurement, D-Q reference frame must be aligned at a fixed position. The Phase-Locked Loop is to solved the situation. If the D-Q reference frame is not fix on a particular frequency, voltages and currents can be variable and composed by several of the frequency. PLL Misalignment can cause the impedance results to be useless. IPFFT improved the accuracy of the impedance model. The data collected from MATLAB and LabVIEW can be read or stored to do post signal processing. The data can be analyzed repeatedly if better algorithm is released later.

Several cases have been tested by MATLAB/Simulink, LabVIEW, and Multisim including passive loads, AC/DC rectifier, AC/DC inverter and AC/DC/AC converter. The results are all posted in chapter 3 and chapter 4.

### **5.3 Future Work and Improvements**

Testing in hardware is still pending. The SPSS lab already has a back to back 3-phase inverter research board made by National Instrument. The voltage and current measurements have built in load and source interface in the research board. The research board picture is shown as Fig 84, and future work and improvements can be done as Fig 84.

#### **5.3.1 Controllable Voltage or Current Source**

In order to do a hardware validation, a controllable voltage or current source which can change frequency from  $10Hz$  to  $10kHz$  is necessary. The magnitude of the injection source should also be changed in order to make appropriate perturbation for different system. Further more, to test an impedance in one particular frequency, each one is injected in two times, each time with different frequency and reverse sequence. As a result, this source should be controlled by MATLAB or LabVIEW in order to automatically inject desired voltages or currents and positive or negative sequence can be controlled as well.

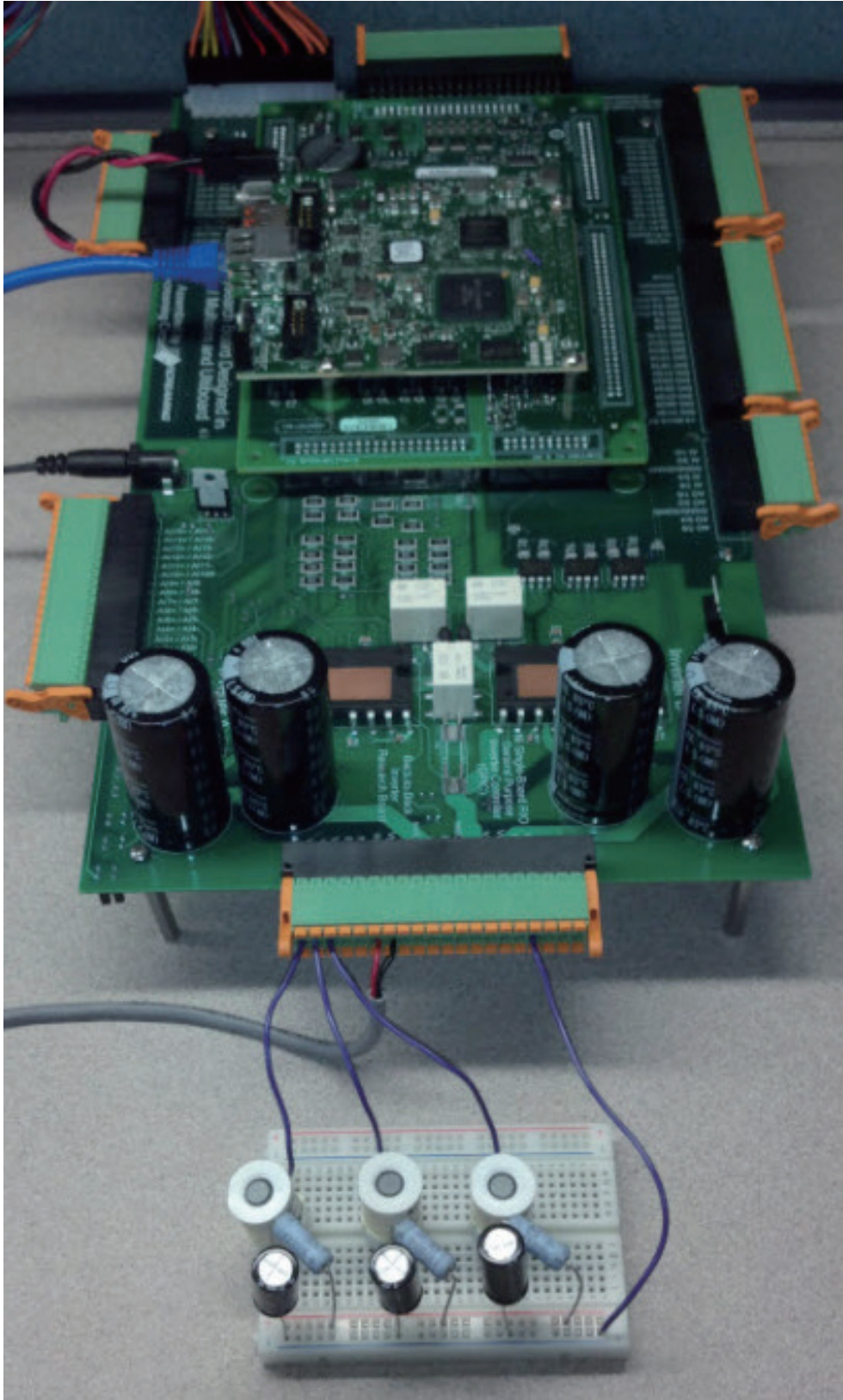


**Figure 83.** Back-to-Back Inverter Research Board with Load



### 5.3.2 Algorithm Implementation

Implement impedance extraction on LabVIEW is not fully completed. FPGA has a huge advantage is that it is useful by its real-time data flow. In LabVIEW algorithm architect, FPGA algorithm is separated in several steps to process the signal. If the FPGA could do the real-time processing, the FPGA algorithm can be as fast as the time to execute in one step. Yet, the main concern of this implementation is given. To collect data as fast as possible, FPGA typically uses fixed-point computation, this method would bring noise into the calculation. Another improvement is, the algorithm of IPFFT should implement in LabVIEW. Since the impedance model cannot be obtained directly form LabVIEW. So far, LabVIEW can only store D-Q voltages and currents data and export to MATLAB to do IPFFT and further analysis. In order to finish impedance extraction automation. IPFFT should transfer to LabVIEW and write into FPGA to do signal process. However, it is not sure if the processor can handle such amount of data acquisition and the effectiveness is another concern.

## References

- [1] M. Belkhat, R. Cooley, and E. Abed, "Stability and dynamics of power systems with regulated converters," in *Circuits and Systems, 1995. ISCAS '95., 1995 IEEE International Symposium on*, vol. 1, Apr 1995, pp. 143–145 vol.1.
- [2] S. Chandrasekaran, D. Borojevic, and D. Lindner, "Input filter interaction in three phase ac-dc converters," in *Power Electronics Specialists Conference, 1999. PESC 99. 30th Annual IEEE*, vol. 2, 1999, pp. 987–992 vol.2.
- [3] Z. Miao, "Impedance-model-based ssr analysis for type 3 wind generator and series-compensated network," *Energy Conversion, IEEE Transactions on*, vol. 27, no. 4, pp. 984–991, Dec 2012.
- [4] M. Sumner, B. Palethorpe, and D. Thomas, "Impedance measurement for improved power quality-part 1: the measurement technique," *Power Delivery, IEEE Transactions on*, vol. 19, no. 3, pp. 1442–1448, July 2004.
- [5] M. Liu, H. Yuan, Y. Sun, and C. Yang, "Research on measurement of dc power supply impedance," in *Electronic Measurement Instruments, 2009. ICEMI '09. 9th International Conference on*, Aug 2009, pp. 2–703–2–706.
- [6] J. Huang, K. Corzine, and M. Belkhat, "Single-phase ac impedance modeling for stability of integrated power systems," in *Electric Ship Technologies Symposium, 2007. ESTS '07. IEEE*, May 2007, pp. 483–489.
- [7] J. Huang and K. A. Corzine, "Ac impedance measurement by line-to-line injected current," in *Industry Applications Conference, 2006. 41st IAS Annual Meeting. Conference Record of the 2006 IEEE*, vol. 1, Oct 2006, pp. 300–306.
- [8] J. Huang, K. Corzine, and M. Belkhat, "Small-signal impedance measurement of power-electronics-based ac power systems using line-to-line current injection," *Power Electronics, IEEE Transactions on*, vol. 24, no. 2, pp. 445–455, Feb 2009.

- [9] J. Huang, "On-line synchronous machine parameter extraction from small signal-injection techniques," in *Power Systems Conference and Exposition, 2009. PSCE '09. IEEE/PES*, March 2009, pp. 1–1.
- [10] Y. Familant, K. Corzine, J. Huang, and M. Belkhat, "Ac impedance measurement techniques," in *Electric Machines and Drives, 2005 IEEE International Conference on*, May 2005, pp. 1850–1857.
- [11] P. Xiao, G. Venayagamoorthy, and K. Corzine, "A novel impedance measurement technique for power electronic systems," in *Power Electronics Specialists Conference, 2007. PESC 2007. IEEE*, June 2007, pp. 955–960.
- [12] G. Francis, R. Burgos, D. Boroyevich, F. Wang, and K. Karimi, "An algorithm and implementation system for measuring impedance in the d-q domain," in *Energy Conversion Congress and Exposition (ECCE), 2011 IEEE*, Sept 2011, pp. 3221–3228.
- [13] Z. Shen, M. Jaksic, P. Mattavelli, D. Boroyevich, J. Verhulst, and M. Belkhat, "Three-phase ac system impedance measurement unit (imu) using chirp signal injection," in *Applied Power Electronics Conference and Exposition (APEC), 2013 Twenty-Eighth Annual IEEE*, March 2013, pp. 2666–2673.
- [14] V. Jain, W. L. Collins, and D. C. Davis, "High-accuracy analog measurements via interpolated fft," *Instrumentation and Measurement, IEEE Transactions on*, vol. 28, no. 2, pp. 113–122, June 1979.
- [15] D. J. Wineland, D. Howe, M. B. Mohler, and H. Hellwig, "Special purpose ammonia frequency standard a feasibility study," *Instrumentation and Measurement, IEEE Transactions on*, vol. 28, no. 2, pp. 122–132, June 1979.
- [16] H. Hikawa and V. Jain, "Jamming canceler using interpolated fft," in *Communications, 1990. ICC '90, Including Supercomm Technical Sessions. SUPERCOMM/ICC '90. Conference Record., IEEE International Conference on*, Apr 1990, pp. 1275–1279 vol.4.

### **About the Author**

Jen-Pin Lin was born in Taipei, Taiwan in June 1, 1988. He received his Bachelor's degree in Electrical Engineering from Chung Yuan Christian University in Taiwan In July, 2010. He worked in Johson Tech Co., Ltd from 2011 to 2012. He studies University of South Florida in Electrical Engineering in Sep 2012 and join Smart Grid and Power System Laboratory in Jul. 2013. He is working on M.S. degree in Electrical Engineering from University of South Florida. His research interests include power electronics, power systems and electrical machinery.